dmj
DIABETES & METABOLISM JOURNAL

Heterogeneity and Clinical Relevance of Human Adipose Stromal and Progenitor Cells

Maxi Albert, Khansa Nalir, Jiawei Zhong, Lucas Massier

Diabetes Metab J 2026;50:217-234 | *https://doi.org/10.4093/dmj.2025.1182*

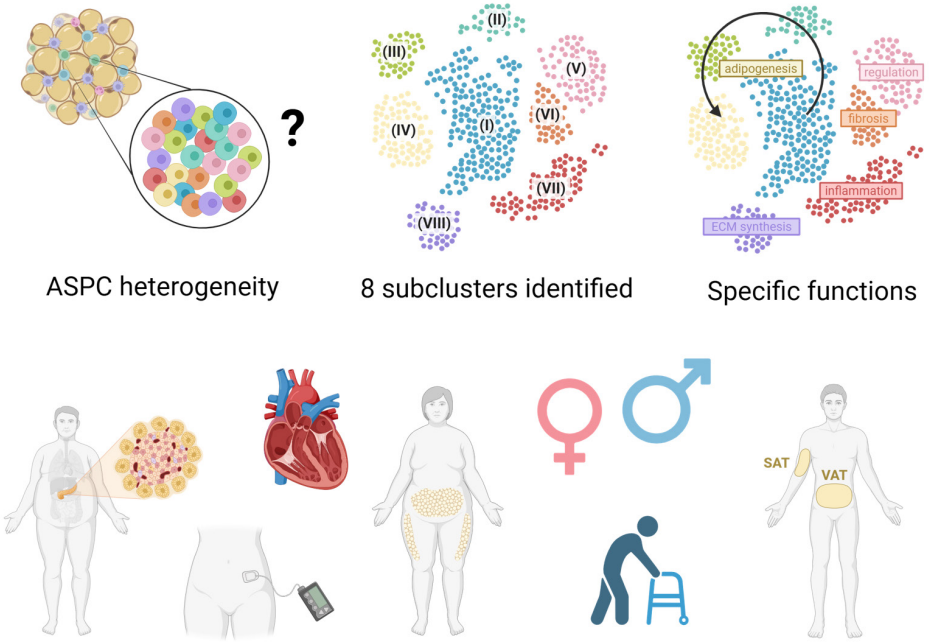

Highlights

- **Single-cell transcriptomic classification delineates 8 distinct ASPC subpopulations**
- **Adipogenic differentiation trajectories characterized 4 subtypes**
- **Subtype abundances are altered in metabolic diseases**
- **Functionally diverse ASPC subclusters associate with metabolic perturbations**
- **Sex, depot origin, age, and metabolic state define ASPC diversity**

How to cite this article:
Albert M, Nalir K, Zhong J, Massier L. Heterogeneity and Clinical Relevance of Human Adipose Stromal and Progenitor Cells. Diabetes Metab J 2026;50:217-234. https://doi.org/10.4093/dmj.2025.1182

Review
Basic and Translational Research
Diabetes Metab J 2026;50:217-234
https://doi.org/10.4093/dmj.2025.1182
pISSN 2233-6079 · eISSN 2233-6087

dmj
DIABETES & METABOLISM JOURNAL

Heterogeneity and Clinical Relevance of Human Adipose Stromal and Progenitor Cells

Maxi Albert[1], Khansa Nalir[1], Jiawei Zhong[2], Lucas Massier[1,2,3]

[1]Helmholtz Institute for Metabolic, Obesity, and Vascular Research (HI-MAG) of the Helmholtz Zentrum München at the University of Leipzig and University Hospital Leipzig, Leipzig, Germany
[2]Department of Medicine (H7), Karolinska Institutet, Karolinska University Hospital, Stockholm, Sweden
[3]LeiCeM-Leipzig Center of Metabolism, Leipzig University, Leipzig, Germany

Adipose stromal and progenitor cells (ASPCs) represent the largest cell population in human white adipose tissue (WAT). Despite their abundance, ASPC heterogeneity remains less well characterized compared to adipocytes or immune cells. Recent single-cell transcriptome studies provide unprecedented resolution of ASPC diversity and function. This review summarizes state-of-the-art approaches, including high-resolution single-cell methods, classical lineage and functional assays, to define ASPC populations. By systematically comparing recent datasets, we identify evidence for at least eight distinct ASPC-subtypes, which demonstrate specific marker genes and putative functional diversity. Along the adipogenic trajectory, these include uncommitted multipotent progenitors, intermediate and committed preadipocytes, and premature adipocytes. Additional populations comprise specialized anti-adipogenic, profibrotic, inflammatory, and fibroblast-like ASPCs. Other cell types are not consistently detected across studies, reflecting both biological and methodological variability, and the need for further validation studies. Better understanding of ASPC heterogeneity may improve the clinical assessment of metabolic disorders and support their treatment. We further discuss subtype-specific (dys)functions linked to fibrosis, inflammation and impaired adipogenesis and describe their increased abundance in metabolic disease. Together, this review integrates current knowledge on ASPC heterogeneity and highlights its clinical relevance, aiming to provide a unified framework for future studies on WAT remodeling and metabolic dysfunction.

Keywords: Adipocytes; Adipogenesis; Adipose tissue; Diabetes mellitus; Fibroblasts; Mesenchymal stem cells; Metabolic diseases; Obesity; Stem cells

INTRODUCTION

Adipose tissue (AT) is a metabolically active and highly heterogeneous endocrine organ. In fact, AT may be regarded as a collection of distinct organs, as humans possess functionally specialized AT depots—most prominently brown adipose tissue (BAT), which drives thermogenesis [1], and white adipose tissue (WAT). Beige AT represents an intermediate state capable of 'browning,' i.e., acquiring thermogenic properties in response to specific stimuli [2]. This review will focus on human WAT.

Within WAT, individual depots can be considered distinct organs in their own right, given their unique developmental origins, cellular composition, and metabolic functions [3,4]. The major WAT depots, subcutaneous adipose tissue (SAT) and visceral adipose tissue (VAT), display divergent endocrine and metabolic profiles, with VAT-dysregulation associated with adverse clinical outcomes [5]. Despite these functional differences, AT across depots shares several key cellular components: (1) adipocytes, (2) immune cells, (3) endothelial cells (ECs), and (4) adipose stromal and progenitor cells (ASPCs). Mesothelial cells represent an additional cell-type found predominantly in VAT [6].

While adipocytes [7], ECs [8], and immune cells [9] have

Corresponding author: Lucas Massier https://orcid.org/0000-0002-6199-2643
Helmholtz Institute for Metabolic, Obesity, and Vascular Research (HI-MAG) of the Helmholtz Zentrum München at the University of Leipzig and University Hospital Leipzig, Philipp-Rosenthal-Straße 27, 04103 Leipzig, Germany
E-mail: lucas.massier@helmholtz-munich.de

Received: Nov. 21, 2025; Accepted: Jan. 28, 2026

been extensively reviewed, ASPCs remain underexplored, despite their critical roles in tissue remodeling, adipogenesis, and metabolic regulation [10-12]. The terminology describing these cells remains inconsistent, with overlapping or context-derived designations including fibroblasts [13-17], preadipocytes [15,18-24], adipose-derived (mesenchymal) stem or stromal cells (AD-MSCs, ADSCs, alternatively adipose stem cells or mesenchymal stem cells) [15,16,20,25-28], adipogenic progenitor cells [4,16,21,23,29-32], and fibro-adipogenic progenitors [23,33-35] have been used to describe overlapping or distinct subsets within the ASPC population. Following the Human Cell Atlas (HCA) consensus [36], we adopt the term ASPCs to describe this heterogenous population.

This review summarizes state-of-the-art approaches for identifying ASPC-subpopulations, outlines recurrent ASPC-subtypes and their functional roles, and discusses the clinical relevance of ASPC dysregulation in metabolic disease.

METHODOLOGICAL APPROACHES FOR STUDYING ASPC

Identification and validation of ASPCs

Traditional methods for ASPC identification

ASPC-subpopulations have classically been studied using immunofluorescence (IF) and fluorescence-activated cell sorting (FACS). FACS allows subpopulation enrichment of primary human samples based on surface markers such as platelet-derived growth factor receptor α (PDGFRα) [37]. Proteomic and transcriptomic profiling enables the identification of subcluster-specific markers, facilitating the targeted isolation of distinct ASPC-subpopulations for functional assays. For example, CD34 has been applied in FACS-based ASPC isolation [25,38]. Although CD34 is typically considered a universal ASPC-marker, emerging research suggests the presence of $CD34^{-}$-ASPCs with beige-like properties [38]. FACS-isolation of intercellular adhesion molecule-1 $(ICAM1)^{+}$-ASPCs revealed two functionally distinct subsets ($CD44^{high/low}$), representing stages along the adipogenic trajectory, with declining CD44-levels towards mature adipocytes [39].

Additionally, immunohistochemical detection of subtype-specific biomarkers enables identification and localization of ASPC-subpopulations. Peroxisome proliferator-activated receptor γ (PPARγ) identifies adipogenic ASPCs via IF [14], while antifibrotic subpopulations were visualized by CD74-labeling [40]. Slit guidance ligand 2 (SLIT2) served as a marker for an EC-colocalized ASPC-cluster [34]. Other examples for subcluster-defining targets include proteoglycan 4 (PRG4), collagen triple helix repeat containing 1 (CTHRC1), CXC motif chemokine ligand 14 (CXCL14), and chitinase-3-like protein 1 (CHI3L1) [28]. Lipid-targeting stains such as Oil Red O and boron-dipyrromethene (BODIPY) were applied to label (pre-)mature adipocytes [41,42].

ASPC identification on single-cell scale

Despite their usefulness, classical approaches lack the capacity to map ASPC-heterogeneity comprehensively. Recent single-cell and spatial approaches revealed a new picture of ASPCs, highlighting them as a major subtype within WAT [24,43-45]. Evaluating transcriptional profiles of single cells permits high-resolution dissection of complex tissues and enables the definition of distinct subclusters within heterogenous tissues, uncovering novel subclusters and differentiation pathways [3,4,16,17,20-23,25,28,30,32,34,35,43,46-53].

While being untargeted, these methods have evident limitations. As adipocytes are too large, buoyant, and fragile for current single-cell approaches, most papers rely either on (1) single-cell RNA-sequencing (scRNAseq) of the stromal vascular fraction (SVF) after collagenase-digestion, or (2) nuclei-isolation and single-nuclei RNA-sequencing (snRNAseq) of the whole tissue. Both methods introduce distinct biases and yield results that do not align well [3,54]. Specifically, scRNAseq provides higher relative abundance and greater resolution of ASPC-subpopulations [34], whereas snRNAseq is preferred due to lower expression of stress-response genes (e.g., *FOS*, *JUN*, *HSP*) and to include adipocytes. However, snRNAseq lacks non-nuclear enriched transcripts, thereby capturing only a fraction of the transcriptome [55] and may underrepresent distinct genes [54]. For both approaches, sample sizes remain limited by cost, and many subpopulations lack validation using established methods and larger cohorts. Nonetheless, these methods provide a high-resolution classification, and recent efforts by the HCA AT-Bionetwork provide a standardized consensus framework [36].

Advanced methods for ASPC identification and validation

Spatial transcriptomics (STx), including spot-based sequencing (i.e., Visium [49]) and *in situ* methods (i.e., Multiplexed Error-Robust Fluorescence *in situ* Hybridization [MERFISH] [56], Xenium [32]), offers alternative approaches to resolve cellular heterogeneity without nuclei- or SVF-isolation. Modern

platforms (i.e., Visium-HD, CosMx, Stereo-seq) now achieve near single-cell spatial resolution [57], however have not been applied to AT yet. Full-length sc/snRNAseq has also been applied to WAT, providing broader gene coverage at lower cell numbers than 3′-based methods and enabling isoform-level analyses [54]. Complementary multi-omics approaches integrate transcriptomic, secretomic, proteomic and genomic data to unravel intercellular regulatory networks within AT [3].

Epigenomic profiling complements ASPC-characterization, focusing on three-dimensional genome mapping [45,58], chromatin conformation [43,45,59], DNA methylation [45, 60], histone modifications [60,61], and subsequent transcriptional regulation utilizing chromatin Immunoprecipitation (ChIP) [61], assay for transposase-accessible chromatin (ATAC)-RNAseq [58,60,62], single-nucleus methyl-3C sequencing (snm3C-seq) [45], cleavage under targets and tagmentation (CUT&RUN/TAG) [60,63], chromosome conformation techniques such as Hi-C [58], and estimation of cell age from single-cell ATAC data using EpiTrace [64].

Together, these technical advances have supported the identification of ASPCs in AT and supported the classification of ASPC-subpopulations with distinct functions.

Computational strategies for ASPC analysis

Computational guides summarize best-practice workflows for single-cell analysis [65,66] and AT-specific considerations [36]. Here, we focus only on aspects relevant to ASPCs.

Data integration minimizes technical variations unrelated to biology. Batch effects arise from differences in sample handling, library preparation, or sequencing platforms. While unnecessary when all data is processed uniformly, integration becomes critical when combining datasets from multiple laboratories. Widely adopted approaches for ASPCs [3,17,20,25,46,51] include Seurat-based methods [67] and Harmony [68]. Benchmarking different algorithms remains good practice to ensure removal of technical effects while preserving biological signal [69]. Reprocessing raw FASTQ-files with consistent pipelines further enhances cross-study comparability.

Given their differentiation potential, ASPC-trajectories can be reconstructed computationally. However, subtypes lacking adipogenic potential should be excluded to avoid misleading lineage inferences. Splicing-based trajectory tools, including Velocyto [70] and scVelo [71], are not applicable to snRNAseq, as it lacks sufficient unspliced transcripts. Velocity-based interpretations in AT-atlases should therefore be treated cautiously. Complementary lineage-tracing approaches, including genetic barcoding and mitochondrial variant tracking, can reveal clonal relationships but remain limited to model organisms for ethical reasons [13,72,73]. Time-resolved RNAseq and pseudotime analysis have delineated differentiation trajectories and progenitor hierarchies within SVF-populations [20,29,34,46].

Cell-cell communication inference in AT follows general frameworks, with CellPhoneDB [74] and CellChat [75] most commonly applied. ASPCs consistently emerged as central communication hubs, acting as both signal senders and receivers [3,21,34,51].

Subtype relevance can be evaluated by correlating proportional abundances with clinical parameters, although limited cohort sizes constrain statistical power. Integrating sc/snRNA-seq with bulk transcriptomics data through deconvolution enhances power and allows meta-analytic validation across cohorts [34]. Similarly, deconvolution of low-resolution STx enables estimation of cell-type composition and spatial co-localization patterns [76].

Marker overlap among subclusters [77] complicates deconvolution. Aggregating transcriptionally similar subtypes, as outlined in Fig. 1A, Supplementary Table 1, reduces this bias.

Functional characterization of ASPCs

Appropriate and well-characterized model systems are essential for investigating ASPC-physiology. Murine and duck ASPC lines like 3T3-L1 [78] and CCL-141 [79] have been established for *in vitro* studies, but their non-human origin limits translational relevance. Human ASPC-generation protocols were published [80], and commercially available human models (human multipotent adipose-derived stem cells [hMADS] [81], Simpson-Golabi-Behmel syndrome [SGBS] cells [82], ASC-52telo [83]) exist, providing more physiologically relevant systems.

Differentiation and functional assays of ASPCs

Multipotent human ASPCs can be *in vitro* differentiated into mature adipocytes [41,84-86], smooth muscle cells (SMCs) [87], extracellular matrix (ECM)-producing fibroblast-like cells [88], immune-regulatory cells [4,89] or myofibroblasts [27], enabling systematic exploration of functional states and lineage flexibility. Further, osteogenic [90] and chondrogenic [91] differentiation pathways were confirmed *in vivo*. Standard gene editing tools (Clustered Regularly Interspaced Short Palindromic Repeats [CRISPR]-Cas9 [92,93], Cre-loxP [14,34,94]),

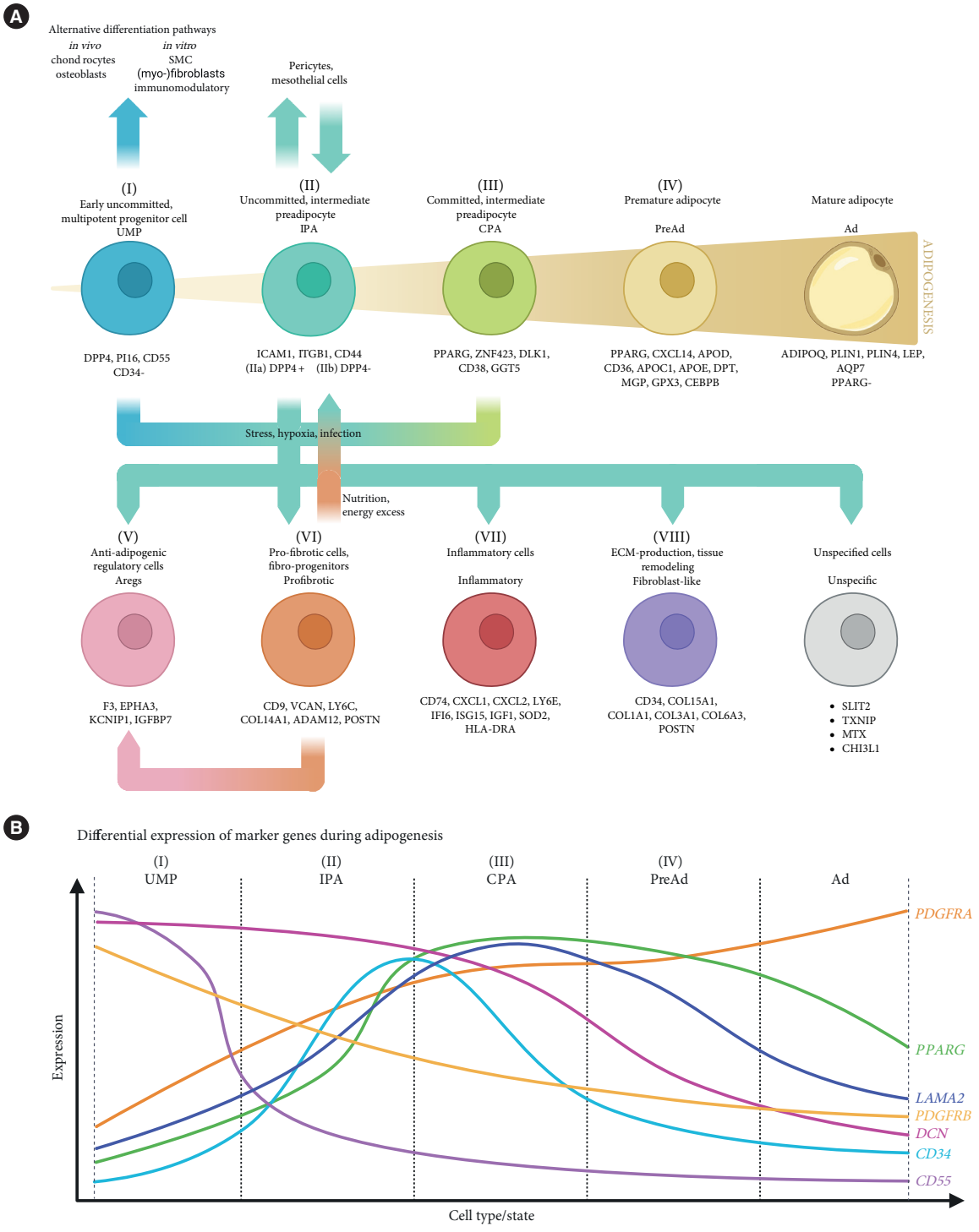

Fig. 1. Overview of identified adipose stromal and progenitor cell (ASPC) subpopulations in human white adipose tissue. (A) Overview of classified ASPC subclusters and respective names, proposed in this review. Cluster-specific marker genes are indicated below the subtype. (B) Conceptual model of differential expression of traditional applied ASPC markers adjusted to adipogenic differentiation states. Data from Whytock et al. [54], Zhu et al. [125], and the adiposetissue.org portal [144] has been used to design the plot. SMC, smooth muscle cell; UMP, uncommitted, multipotent progenitor cell; IPA, intermediate preadipocyte; CPA, committed, intermediate preadipocyte; PreAd, premature adipocyte; Ad, adipocyte.

have been applied to ASPCs for perturbation studies and lineage tracing, clarifying differentiation pathways *in vivo* and *in vitro* [13,72]. These models support mechanistic and high-throughput studies but cannot reproduce the native WAT-microenvironment. Patient-derived cells and FACS-isolated subpopulations remain the most physiologically relevant approach.

ASPC-subclusters can be interrogated using assays tailored to their putative, subtype-specific roles. Classical fibroblast-like states can be assessed by ECM secretion [10], fibrotic gene expression, immunomodulation [95], and wound healing capacity [96,97]. Adipogenic potential is evaluated by lipid accumulation and adipocyte marker expression (e.g., perilipin-1 [*PLIN1*]; adiponectin [*ADIPOQ*]) [85,98]. *CD34*-expression can further distinguish adipocyte subtypes with divergent lipid turnover and thermogenic capacities [38]. Additional assays capture myofibroblast differentiation [99], angiogenic potential [100,101], and paracrine immunomodulation [38,102]. Metabolic assays, focusing on thermogenesis [2] and mitochondrial activity [29,103,104], provide complementary insight into energetic states. Spatial metabolomics and matrix-assisted laser desorption/ionization mass spectrometry (MALDI-MS) imaging have been adapted for WAT to visualize metabolic and lipidomic heterogeneity [105,106]. Together, these readouts allow functional annotation of subclusters and integration of molecular signatures with biological phenotypes.

Advanced ASPC model systems

These technological advances have expanded our understanding of AT-heterogeneity, yet models better recapitulating the native microenvironment are required. Coculture systems incorporating ECs [107,108], dermal fibroblasts [95] and macrophages [102] have improved functional characterization, revealing that ASPCs can promote angiogenesis [100,109] enhance ECM production [10,50] and reduce expression of classical fibroblast marker genes [95]. Murine AT-organoids derived from SVF, including immune populations, have enabled investigation of lipid metabolism and immune-adipocyte crosstalk [110] and pre-vascularized human beige AT-organoids have recently been established [111]. Embedding ASPCs into growth factor-reduced matrigel promotes differentiation into unilocular adipocytes with enlarged lipid droplets, facilitating studies of adaptive AT-expansion and precursor heterogeneity [112]. Human AT-derived organoids show substantial potential for tissue engineering and regenerative applications [113] and may be further improved by incorporating donor-specific variability and standardized functional readouts. Recent reviews have summarized these advances and their translational relevance [114]. Finally, transplantation of human ASPCs into immunocompromised mice provides an additional avenue to examine functional properties *in vivo* [115].

FUNCTIONALITY AND CELLULAR HETEROGENEITY OF HUMAN ASPC

ASPCs function as adipogenic precursors, regulate ECM production and remodeling, and modulate local inflammation. Dysregulation of these processes contributes to fibrosis, chronic inflammation, and maladaptive ECM remodeling [10,116]. While these general roles are established, the functional specificity of individual ASPC-subclusters remains unclear.

To address this, we integrated published sc/snRNA-seq datasets to derive consensus ASPC signatures (Supplementary Table 1), identifying eight recurrent subtypes (Fig. 1A). Below, we outline the rationale for this classification and highlight key subtype-specific functions.

Heterogeneity of ASPCs

General ASPC markers

To isolate ASPCs from other cell types, several general markers are commonly used, including platelet-derived growth factor receptor alpha (*PDGFRA*) [17,20,23,25,28,35,46,49,50,53,117], *PDGFRB* [21,25,30,34], decorin (*DCN*) [25,28,47,49,50,52,53], laminin subunit alpha 2 (*LAMA2*) [23,49], integrin subunit beta 1 (*ITGB1*; *CD29*) [21,28], *THY1* (*CD90*) [28,50,51] and *CD34* [4,17,22,28,34,50,51]. Most studies rely on *PDGFRA* and *CD34*, although both show subtype-specific variation: *PDGFRA*-expression increases during adipogenesis [20,24,32,46,48,54,118], while *CD34* marks fibroblast-like ASPCs with higher stemness [17,21,28,48,52], and *CD34*$^{-}$-ASPCs tend to be more committed to adipogenic differentiation [38,46]. *THY1* is used as a general ASPC-marker [28,50,51], yet other studies identified it as a subtype-specific marker across depots [25,30,35,46,49,54]. Similarly, *DCN* is sometimes applied broadly but appears enriched in ASPCs with high differentiation potential [24,25,32,48,54]. Overall, several markers historically treated as 'general' ASPC identifiers likely capture only subsets of the full ASPC compartment, most notably *CD34* and *DCN*.

Classification of adipogenic ASPCs

The first well-defined cluster is identified by expressing dipep-

tidyl peptidase 4 (*DPP4*; *CD26*) [3,20,21,23,25,28,30,32,34,46,47,49,50,52-54], *CD55* [3,17,20,23,25,28,30,32,34,35,46,49-52,54] and peptidase inhibitor 16 (*PI16*) [3,17,20,21,23,30,34,35,47,49,51,54], referring to early uncommitted, multipotent progenitor cells (UMP) (I). *DPP4* has been widely used to isolate progenitors for downstream applications, i.e., differentiation [50,119,120]. ASPCs have also been identified by *PRG4* [3,4,20,21,28,35,49,52,54,56,121], which is a major player in wound healing and thus might refer to anti-fibrotic functions, being not a suitable marker for UMPs. Recently, an ASPC-subcluster was defined by high expression of *DPP4*, *ITGB1*, *THY1*, and *CD9* [46], likely referring to a profibrotic cluster with high differentiation potential. Further, the *CD9*$^+$ subpopulation was identified as an intermediate state between UMPs and more differentiated cells [51]. We assume that *CD9*$^+$ and *PRG4*$^+$ clusters may overlap, displaying an early progenitor of pro-inflammatory mediators.

Another subcluster can be identified by *ICAM1*-expression [20,21,23,30,35,48,50-52]. This uncommitted, intermediate preadipocyte (IPA) cluster (II) can be further subdivided by *DPP4*-expression decreasing along adipogenesis [20,21]. More committed precursors can be defined by *PPARG*-expression [17,20,23,25,28,30,32,34,36,46,48,50] and more adipose-specific markers, such as *CD38* [25,54], gamma-glutamyltransferase 5 (*GGT5*) [28,30], zinc finger protein 423 (*ZNF423*) [25,54], delta like non-canonical Notch ligand 1 (*DLK1*) [25,54], apolipoprotein C1 (*APOC1*) [20], *APOD* [3,4,12,16,20-22,24,28,34,35,48,49,52,54], *APOE* [4,16,20,28,30,35,50,52], fatty acid binding protein 4 (*FABP4*) [4,16,20,34,47-50], CCAAT enhancer binding protein beta (*CEBPB*) [4,35,56], matrix Gla protein (*MGP*) [4,16,22,24,28,34,49,52,54], *CD36* [4,12,16,17,20,22,23,52,53], *CXCL14* [3,4,12,16,21,22,24,28,34,35,49,52-54,56] and complement factor D (*CFD*) [4,16,22,34,48,49,52-54,56]. Those marker genes vary in their expression along adipogenic differentiation and further subtypes might be identified. Here, we define two ASPC-subtypes: (III) committed, intermediate preadipocytes (CPA) and (IV) premature adipocytes (PreAd). CPAs already exhibit adipocyte-related gene expression, e.g., *PPARG*, and are therefore considered 'committed.' But we assume that alternative differentiation pathways can be induced in CPAs, similar to UMPs and IPAs. In contrast, PreAds are more strictly committed to the adipogenic line and express specific genes, i.e., *APOD*, *CXCL14*, and *CD36* or even *ADIPOQ*. Gene enrichment analysis defines main functions in triglyceride metabolism pointing to adipogenic commitment [28]. Furthermore, depot-dependent PreAd-markers were reported. For instance, *APOE* was enriched in *APOD*$^+$ *CXCL14*$^+$ PreAd in SAT [16,28,52], but found enriched in non-PreAd subclusters in VAT, i.e., in a fibro-progenitor/adipogenic regulatory cell (Areg)-like [35] and a retinol binding protein 5 (*RBP5*)$^+$ ASPC-cluster [20]. *CD36* was identified in SAT-PreAds across studies [4,23,52,53] and was reported in VAT-Aregs [23] and fibro-progenitor-like ASPCs in perivascular AT (PVAT) [34]. Enriched glutathione peroxidase 3 (*GPX3*)-expression was demonstrated in VAT-PreAds [4] and in a *APOD*$^+$-cluster in creeping fat [48] but not in SAT. In addition, some identified CPA and PreAd markers, such as *FABP4*, *CEBPA*, and *S100A4*, appear to be very unspecific and are inappropriate for defining PreAds or other ASPC-subclusters.

Contrary, adipogenesis is inhibited by a specific ASPC-cluster being responsive to external stimuli: anti-Aregs (V) are identified by expressing *F3* (*CD142*) and EPH receptor A3 (*EPHA3*) [3,20,23,25,32,50-53] and also regulate angiogenesis and immune responses [3,20,50,51,89].

Non-adipogenic ASPC-subtypes

Apart from adipogenesis, we define functionally diverse subtypes: profibrotic, inflammatory, and fibroblast-like. Profibrotic fibroblast-precursors (VI) are marked by the expression of *CD9*, versican (*VCAN*), and *LY6C* [26,28,32,35,46,49,51,54,56]. This alternative differentiation pathway is regulated by PDGFRα, acting as a molecular switch [88,94]. Intermediate states from UMPs to *CD9*$^+$-ASPCs were confirmed [46,51]. Spatial mapping locates this subcluster in a profibrotic niche within WAT [34]. A pro-inflammatory subtype is marked by *CD74*, *LY6E*, and interferon alpha inducible protein 6 (*IFI6*) (VII) and induces immune responses via cytokine secretion (CXCL1, CXCL2) or distinct pathway signaling [3,4,34,52,54,56]. This cluster may compromise functionally distinct subsets [4,34,52], although evidence remains limited. Precisely, antifibrotic and immunomodulatory activity of *CD74*$^+$-ASPCs has been reported by elevated secretion of fibroblast growth factor 2 (FGF) and hepatocyte growth factor (HGF) [40]. ECM-production and tissue remodeling is mainly exhibited by a *CD34*$^+$-subcluster (VIII) that is additionally identified by expressing collagens (*COL15A1*, *COL1A1*, *COL3A1*, *COL6A3*) [4,17,20,25,32,34,47-49,54,56]. This subcluster strongly contributes to AT-remodeling during weight loss (WL) or gain, or after disease recovery. We assume that clusters (VI–VIII) can either differentiate from UMPs, IPAs, or CPAs or from each other.

Only few studies, primarily in mice, showed non-adipogenic differentiation of ASPCs. In fact, transforming growth factor beta (TGFβ)-treatment of *Pdgfra*$^{+}$-ASPCs in mice led to increased expression of fibrosis markers leading to ECM-synthesizing *Cd9*$^{+}$-ASPCs, a combination of our clusters (VI) and (VIII) [88]. In human UMPs, TGFβ-treatment induced differentiation towards cluster (VIII) [10] and reduced cluster (VII) activation [40], along with adipogenesis inhibition [30,122]. *Pdgfra* enhances mechanistic target of rapamycin (mTOR) signaling and induces the differentiation into ECM-synthesizing cells, corresponding to our cluster (VIII) [94]. UMPs differentiate into DPP4^{-}-myofibroblasts upon TGFβ stimulation and subsequent Hippo pathway activity, increasing AT fibrosis and being connected to cluster (VII) [120]. In humans, a reversible differentiation pathway towards ECM-expressing, progenitor-like cells (structural Wnt-regulated AT-resident [SWAT] cells, putative intermediate state towards (VIII)), is induced by transient Wnt-signaling [29,123]. Moreover, functionalities may overlap, e.g., inflammation and profibrotic signaling contribute to obesity-induced AT fibrosis [11,88,94,124].

Conclusion of proposed ASPC classification

Collectively, eight distinct ASPC-subtypes are defined: (I) UMP, (II) IPA, (III) CPA, (IV) PreAd, (V) Aregs, (VI) fibro-progenitors (profibrotic), (VII) immunomodulatory cells (inflammatory), and (VIII) ECM-producing cells with tissue remodeling capacity (Fibroblast-like). These subclusters are commonly identified by specific marker genes: (I) *DPP4*, *CD55*, *PI16* [3,20,46,47,51], (II) *ICAM1*, *ITGB1*, *CD44* [3,30,51], (III) *PPARG*, *ZNF423*, *DLK1*, *CD38* [25,28,30], (IV) *PPARG*, *CXCL14*, *APOD*, *CD36* [4,12, 22,23,28,30,34,49], (V) *F3*, *EPHA3* [3,30,46,51], (VI) *CD9*, *VCAN*, *LY6C* [26,32,35,49], (VII) *CD74*, *CXCL1*, *LY6E* [4,34], and (VIII) *CD34*, *COL1A1*, *COL6A3*, *COL15A1* [4,32,47,51] (Fig. 1).

However, more subpopulations can be defined, depending on varying computational cutoffs, e.g., when setting the resolution to separate clusters. For the following subtypes, there is only evidence from isolated studies: ferroptosis suppressor protein 1 (*FSP1*)$^{+}$-ASPCs support the maintenance of adipocyte differentiation potential of adjacent PreAds but are not capable of adipogenesis themselves [14]. Thioredoxin-interacting protein (*TXNIP*)$^{+}$-ASPCs have been associated with strong metabolic pathway enrichment and high differentiation potential [16] and were identified across SAT, VAT, and PVAT [34]. STx-data indicated proximity of *SLIT2*$^{+}$-ASPCs to blood vessels [34] and *SLIT2* in ECs has been reported to be affected by obesity [109], suggesting a putative angiogenesis-regulating function of this ASPC-subtype. MTX-ASPCs show increased metallothionein-expression (*MT1X*, *MT1A*, *MT2A*, *MT-RNR1*) and may reflect on a stress-responsive subtype [4,20,28, 34,35,52]. Further meta-analyses across depots and diseases comparing data from scRNAseq and snRNAseq are required for a comprehensive overview.

Differentiation and functional characterization of ASPC-subtypes

ASPC with adipogenic differentiation potential

ASPCs are reported to be the prevailing adipocyte progenitor in both BAT and WAT [13]. Differentiation of human pluripotent stem cells into adipocytes has been described utilizing PPARγ, CEBPB, PR domain containing 16 (PRDM16) [82,84]. Recent scRNAseq-studies have revealed UMPs as a common progenitor of adipocytes and ASPC-subclusters, being Wnt-regulated and showing enrichment in ECM-production and developmental genes [29]. Other differentiation pathways may be exhibited in response to various stimuli.

During adipogenesis, UMPs differentiate into IPAs, CPAs, and PreAds, along multiple intermediate states, before reaching the state of mature adipocytes (Fig. 1) [125]. Other progenitors, such as pericytes [126], mesothelial cells (via insulin like growth factor binding protein 2 [*IGFBP2*]$^{+}$-intermediate state) [20] and SMCs [87], can, however, likewise serve as progenitors for adipocytes. In contrast, other differentiation pathways may be followed by adipogenic ASPC-subtypes, leading to the formation of clusters (V–VIII) and thus inhibiting adipogenesis, i.e., via Areg activity [23,89]. Enhanced PDGFRα-activity may lead to the differentiation of adipogenic ASPCs (UMP, IPA, CPA) or to formation of clusters (VI–VIII) [94]. Further, Aregs and IPAs can arise from the profibrotic *CD9*$^{+}$-population too [51]. UMPs [30,34,127] and profibrotic ASPCs [34,88] are sensitive to TGFβ-signaling and subsequent adipogenesis inhibition. IPA and CPA are associated with cellular responses to various stimuli, including mechanical stress, FGF and calcium signaling, regulating adipogenesis [51]. Activating the Wnt/β-catenin pathway inhibits adipogenic commitment [128] and distinct mutations have been shown to promote obesity [129] and type 2 diabetes mellitus (T2DM) [130]. Adipogenic commitment can be further regulated via obesity-induced senescence [131,132], gremlin 2, DAN family BMP antagonist (*GREM2*)-overexpression in aging [133], mitochondrial me-

tabolism [134], genetic variants such as LDL receptor related protein 5/6 (*LRP5/6*; Wnt-coreceptors) [135], and anti-adipogenic substances, i.e., retinoic acid [136], microRNAs [137], and inflammatory cytokines [42].

Proposed functional roles of ASPC-subclusters

ASPCs are the major players of ECM remodeling and AT structure integrity [10,11,15]. This dual role of, either adipogenic differentiation capacity or structural integrity as main function, has been confirmed previously [15,29]. Specifically, UMPs, Aregs and profibrotic ASPCs have been implicated in ECM organization [51]. Further functions include WAT beiging among exposure to cold or adrenalin signals [13], regulation of lipid and cholesterol metabolism [25], cell-cell communication [11] and inflammation [138]. However, ASPC-subpopulations vary in ECM-related gene expression, adipogenic commitment metabolic signatures [25] as well as angiogenesis regulation [50]. To some extent, those functions may be associated with specific ASPC-clusters, e.g., immunomodulatory responses may be correlated with clusters (VI) and (VII) [4,54]. But, as subcluster classification is inconsequent across studies, functional annotations may only be speculated on, and further meta-analysis is required. Moreover, depot- and disease-specific shifts in ASPC-populations suggest functional relevance for metabolic health, which will be addressed in the next chapter.

CLINICAL IMPLICATIONS OF ASPC HETEROGENEITY

ASPCs are the most abundant cell class in AT and play essential roles in AT-remodeling and metabolic regulation (Fig. 2A). Their abundance and functional state are linked to depot and metabolic health, suggesting that specific ASPC-subtypes may contribute differently to obesity, insulin resistance, and fibrosis. Emerging sn/scRNAseq-studies revealed both shared and depot-specific responses to metabolic stress. Despite inconsistencies among studies, an emerging picture suggests: ASPCs adapt dynamically to local and systemic metabolic cues, and their dysregulation may represent an early cellular correlation with metabolic dysfunction.

Inverse regulation of SAT and VAT ASPCs

WAT-depots, such as SAT and VAT, exhibit distinct functions and could be considered as functionally distinct organs. This depot-specific specialization extends to their ASPC-compartments. Reinisch et al. [23] observed a lower overall abundance of ASPCs in SAT from metabolically unhealthy obese (MUO) individuals, consistent with findings by Loft et al. [53], who reported an enrichment of SAT-ASPCs following bariatric surgery-induced WL. Similarly, Kar et al. [44] noted a reduction in ASPC-proportions upon impaired adipogenesis, linked to altered expression of genes associated with both obesity and aging. In contrast, Emont et al. [3] found a positive correlation between ASPC-abundance and body mass index (BMI) in SAT.

In VAT, ASPC levels were increased in MUO [23], whereas Emont et al. [3] reported a negative association between VAT ASPC abundance and BMI. Metabolically, gluteofemoral ASPCs were enriched in lipid and cholesterol metabolism pathways, and displayed high proliferative potential, while abdominal ASPCs were more preadipocyte-committed and enriched for ECM and ribosomal gene expression [25]. Subtype-level comparisons further highlight these depot-specific differences: UMPs, in line with their ubiquitous cross-organ relevance as multipotent progenitors [139], were shown to be similarly abundant across multiple depots, while IPAs, CPAs, and PreAd were more depot-specific [139]. The latter, as well as Aregs, were found to be more abundant in SAT versus VAT [3,4,16].

Despite some discrepancies, collective evidence supports inverse regulation of ASPC-abundance and differentiation potential in SAT versus VAT, linking depot-specificity to metabolic health (Fig. 2B).

ASPC subtype abundance reflects metabolic state

Emont et al. [3] and Massier et al. [34] reported a positive correlation between UMPs and BMI, supported by Loft et al. [53], who observed a decline in UMP abundance following WL. Given that adipocyte number is largely established during childhood [140], an expanded UMP pool may predispose to increased adiposity by enhancing the capacity for lipid storage (Fig. 2C).

Following the adipogenic trajectory, *TXNIP*$^{+}$-ASPCs (PreAds/fibroblast-like) have been negatively correlated with BMI [34], in line with more recent data that reported increased *PPARG*$^{+}$-IPAs/CPAs after WL [53]. Conversely, abundance of *CXCL14*$^{+}$-PreAd declined following WL [53], consistent with Emont et al. [3], who found Aregs and ASPCs expressing sarcoglycan zeta (*SGCZ*), *PIEZO2*, twist family bHLH transcription factor 1 (*TWIST1*) positively associated with BMI [3]. Cluster (VII) (inflammatory ASPCs) was more abundant in

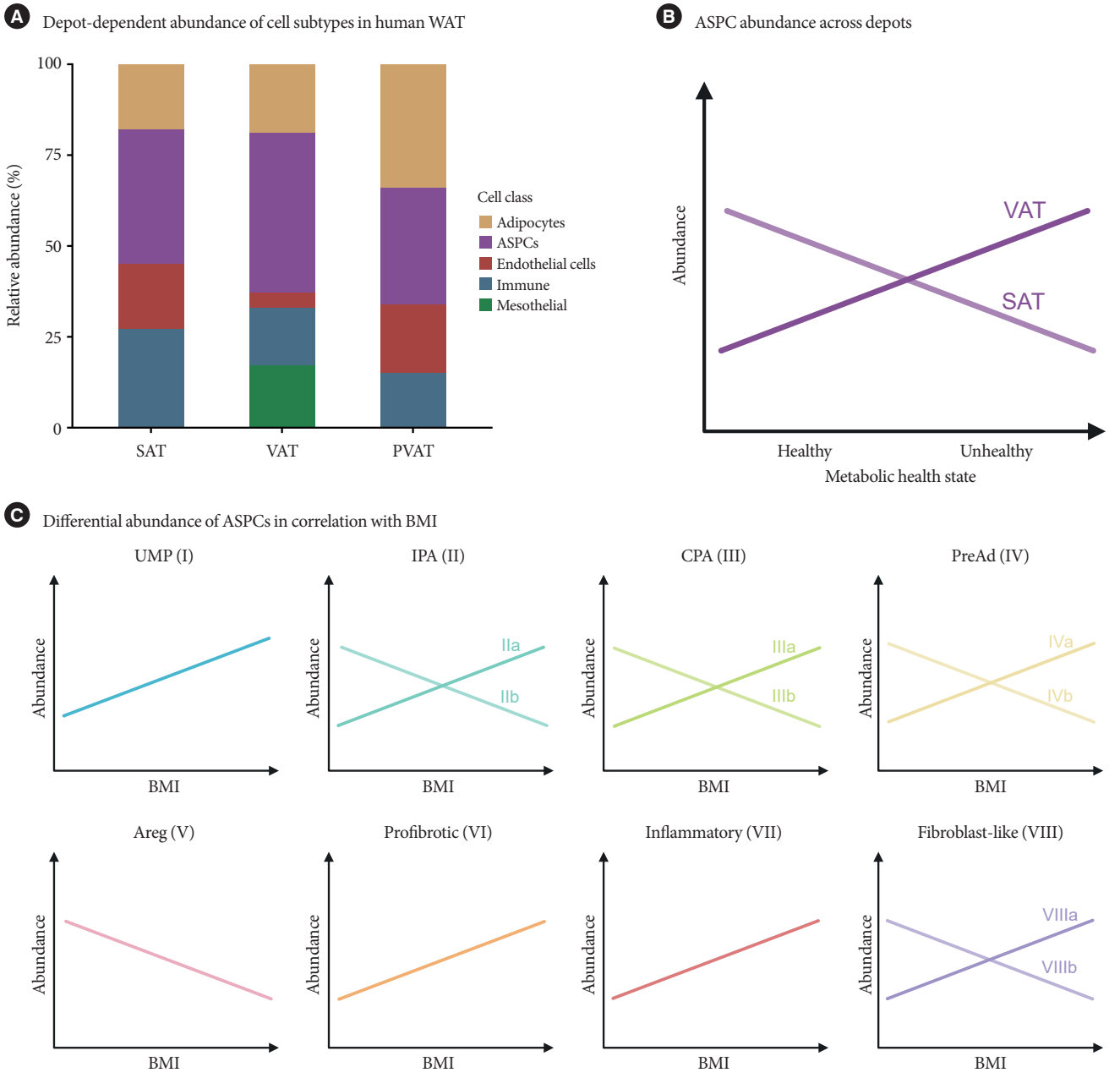

Fig. 2. Depot-specific abundance of adipose stromal and progenitor cells (ASPCs) and clinical correlation of ASPC heterogeneity. (A) ASPC proportions across white adipose tissue depots. Data from Massier et al. [34] and Jalkanen et al. [76]. (B) Overall ASPC abundance across subcutaneous adipose tissue (SAT) and visceral adipose tissue (VAT), in line with Reinisch et al. [23]. (C) Conceptual model of subtype abundance correlated to body mass index (BMI). Data from Liu et al. [28], Emont et al. [3], Massier et al. [34] and Loft et al. [53] was utilized to design this figure. PVAT, perivascular adipose tissue; UMP, uncommitted, multipotent progenitor cell; IPA, intermediate preadipocyte; CPA, committed, intermediate preadipocyte; PreAd, premature adipocyte.

breast AT in young women, pre-menopause, and obesity [56]. This apparent dichotomy between ASPC-states is mirrored in metabolic health: Reinisch et al. [23] identified PreAds (*CD36*$^{+}$, *PPARG*$^{+}$) enriched in metabolically unhealthy obesity (MUO) versus metabolically healthy obesity (MHO) and IPAs (*ICAM1*$^{+}$, low density lipoprotein receptor [*LDLR*]$^{+}$) reduced in the same cohort [23].

Beyond adipogenesis, PreAds contribute to complement ac-

tivation, serving as a major source of circulating CFD (CFD/adipsin) [22,34,48,53]. Additionally, PreAds secrete further regulators of the alternative complement pathway (C3, complement factor H [CFH]), and downstream complement-associated factors (APOD, gelsolin [GSN], CXCL14, CXCL12) [24,56]. In contrast, UMPs secrete CD55, an inhibitor of C3-C3b conversion, thereby inhibiting the complement cascade [141]. UMPs display immunoregulatory responsiveness, reacting to chemokines (CCL2, CCL5, CXCL1, CXCL2, CXCL8), and cytokines (TNFα, interleukin 1 beta [IL1β], IL-15), linking ASPCs to AT-inflammation and metabolic deterioration [4,22,35,52,56,142,143]. Elevated stress-response signaling (*FOS*, *JUN*, signal transducer and activator of transcription 3 [*STAT3*]) in UMPs, IPAs and PreAds in obesity, with reversal after WL, further supports the role of ASPCs in healthy AT-remodeling [17,32,53].

Taken these findings together, Aregs showed a negative correlation with BMI whereas clusters (I), (VI) and (VII) were positively correlated. The remaining clusters exhibited either positive or negative associations with BMI or no demonstratable correlation (Fig. 2C).

Specialized and adaptive ASPC states

Beyond their role in adipogenesis, ASPCs acquire distinct functional states that sustain ECM integrity and maintain AT-homeostasis. Under inflammatory or metabolic stress, they can acquire antigen-presenting features characterized by major histocompatibility complex (MHC) class II expression (major histocompatibility complex, class II, DR alpha [*HLA-DRA*], *HLA-DRB1*, *HLA-DRB5*) [4,28,34,52] or adopt macrophage-like profiles [4,22,34,35]. Functional validation of these states, however, remains limited. Evidence from mouse studies showed polarization into keratin 23 (Krt23)$^+$-ASPCs, secreting CCL2, CCL6, and CCL9 and recruiting neutrophils and macrophages [144]. Persistent dysregulation of fibroblast-like ASPCs may further promote pathological fibrosis through excessive ECM deposition and remodeling.

Positively BMI-correlated ASPC-subclusters, such as UMPs [21], Aregs [3], CD83$^+$ [24], and IGFBP2$^+$ [20], display adaptive states responding to metabolic health: WL leads to reduced hypoxia and decreased expression of profibrotic (*TGFB*) and anti-adipogenic genes (*WNT*), particularly in PPARG$^+$-ASPCs [32]. Further, IPAs and profibrotic ASPCs were elevated in T2DM and obesity [51].

Community databases such as the AT Knowledge Portal (adiposetissue.org) enable clinical association analyses of subtype-specific marker genes, revealing substantial heterogeneity even within defined clusters (Fig. 3) [145]. Notably, adaptive, inflammatory and profibrotic subtypes show the strongest correlations with homeostatic model assessment of insulin resistance, triglyceride levels, adipocyte volume, BMI, waist-to-hip ratio, and circulating inflammation, measured by C-reactive protein. Depot-level comparisons further suggest weaker clinical associations for VAT-specific markers, implying depot-specific roles in tissue adaptation and a more pronounced dysregulation of SAT-ASPCs with adverse clinical parameters. These trends should be interpreted cautiously, given the predominance of SAT-derived datasets.

Sex-dependent ASPC differences in adipose distribution and function

Sexual dimorphism is a major determinant of AT distribution and metabolic disease risk [146]. Emerging evidence indicates contribution of ASPCs to these sex-specific differences. A female-specific Areg polarization occurred exclusively in MUO women [23]. This might explain conflicting findings on Areg abundance, being increased [3] or decreased [51] upon obesity.

Further evidence for sex-linked ASPC-specialization comes from depot-specific analyses revealing that PPARγ phosphorylation status differs between inguinal depots of men and premenopausal women [140], suggesting sex-specific regulation of adipogenic signaling. Moreover, ASPC-subclusters isolated from infrapatellar fat pads exhibit transcriptional differences associated with both local inflammation and sex [46]. Collectively, these findings point towards sex-specific ASPC-transcriptomes that may underlie the well-recognized differences in fat distribution and metabolic flexibility between men and women. Nevertheless, systematic functional studies in human cohorts remain scarce. A better understanding of sex-dependent ASPC-biology could illuminate the cellular basis for divergent cardiometabolic risks observed between women and men and identify new opportunities for individualized therapeutic strategies.

ASPC aging and cellular senescence impair regenerative and metabolic function

Aging profoundly alters the abundance and functionality of ASPCs, contributing to impaired AT-plasticity and metabolic decline. Evidence from both *in vitro* and *in vivo* studies indicates ASPCs progressively acquiring senescent features with

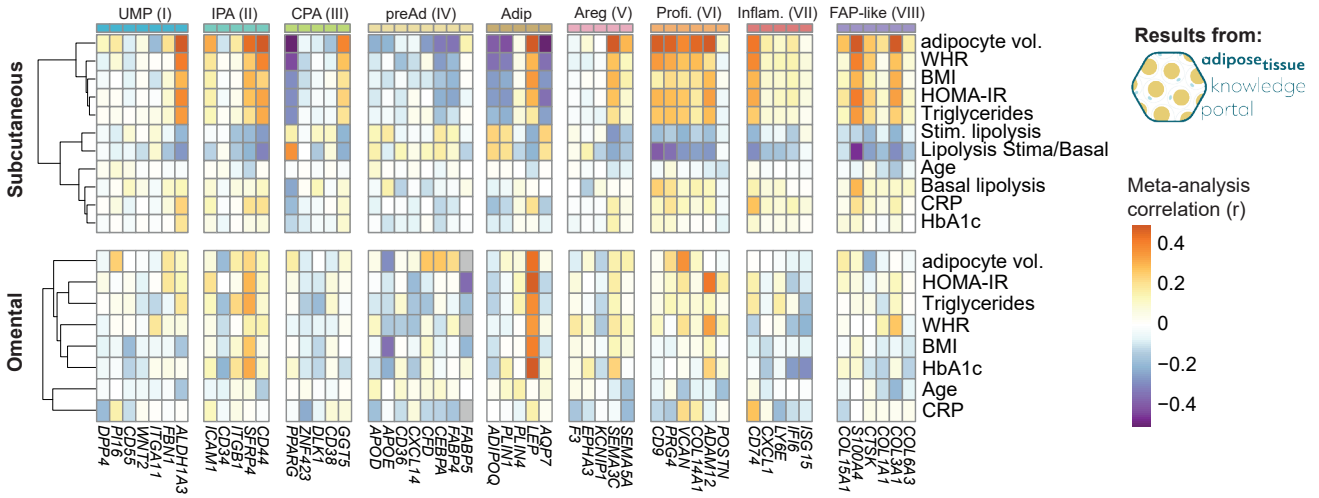

Fig. 3. Correlation of adipose stromal and progenitor cell (ASPC) subtype specific marker genes across human white adipose tissue depots with clinical parameters. Data was obtained through the adipose tissue knowledge portal [144], meta-analysis correlation across all cohorts in the portal was extracted through the clinical module (https://adiposetissue.org/clinical) and visualized. UMP, uncommitted, multipotent progenitor cell; IPA, intermediate preadipocyte; CPA, committed, intermediate preadipocyte; PreAd, premature adipocyte; Areg, adipogenic regulatory cell; FAP, fibro-adipogenic progenitor; WHR, waist-to-hip ratio; BMI, body mass index; HOMA-IR, homeostatic model assessment of insulin resistance; CRP, C-reactive protein; HbA1c, glycosylated hemoglobin.

age. In cultured SAT-derived ASPCs, Mitterberger et al. [147] reported classical senescence characteristics, including enlarged, flattened morphology, elevated β-galactosidase activity and reduced adipogenic potential. Similarly, Choudhery et al. [148] demonstrated that ASPCs from older individuals display reduced proliferative capacity, fewer population doublings, and higher senescence marker expression compared with those from young donors. Aging also compromises the paracrine support of ASPCs: senescent cells secrete lower levels of angiogenic factors, resulting in impaired endothelial network formation [148]. At transcriptomic level, Maredziak et al. [149] found that while the global gene-expression profile of aged ASPCs remains relatively stable, specific changes occur in cell-cycle regulators, accompanied by a shortened G1 phase and increased nascent protein synthesis.

In vivo data confirmed aging-related loss of ASPC-abundance and -functionality. Kar et al. [44] reported a significant decline of SAT-ASPC abundance with age, an effect most evident in lean individuals. Interestingly, obesity appeared to abolish the typical age-related decline, as young obese participants already displayed low ASPC-levels comparable to those of older adults, suggesting that obesity induces a premature aging phenotype. The same study identified an age-dependent gene network linking ASPC-loss to impaired adipogenesis and metabolic dysfunction, highlighting potential therapeutic targets to mitigate obesity-related AT-deterioration [44].

OUTLOOK

Collectively, current evidence indicates that ASPCs constitute a highly adaptive and plastic cellular compartment that dynamically responds to local tissue demands and systemic metabolic cues. Despite the rapid expansion of single-cell studies, many ASPC-subclusters, particularly those reported in only one or a few datasets, remain insufficiently validated across independent cohorts. While the lack of replication may reflect technical artefacts or differences in bioinformatic pipelines, it may equally arise from cohort-specific factors such as depot origin, metabolic state, age, or sex. Resolving these ambiguities will require larger, well-powered studies employing standardized and multiplexed single-cell and spatial profiling approaches across diverse human populations.

A major limitation of the current literature is the limited spatial context for most ASPC-subtypes. Understanding how ASPC-subpopulations are organized within AT, how they relate to vasculature, immune cells, and adipocytes, and how these spatial relationships change in disease states will be essential for assigning functional relevance. High-resolution STx

and integrated multi-omic approaches are therefore expected to play a central role in future investigations.

Beyond descriptive profiling, the field must increasingly focus on functional characterization. ASPCs exhibit remarkable plasticity, yet their differentiation trajectories, lineage hierarchies, and context-dependent fate decisions remain incompletely defined. In this regard, lineage-tracing and perturbation experiments in model organisms will remain indispensable for establishing causality and dissecting regulatory pathways that cannot be resolved from human observational data alone.

From a translational perspective, a critical open question is whether ASPC-subpopulations differ in their responsiveness to pharmacological or lifestyle interventions. It remains unclear whether distinct subtypes share common receptor repertoires and signaling pathways or whether selective modulation of specific ASPC states is feasible. Addressing this question could open new avenues for targeted therapies aimed at restoring healthy AT-remodeling, improving adipogenic capacity, or limiting fibrosis and inflammation in metabolic disease.

Finally, ASPCs should not be studied in isolation. Their phenotype and function are shaped by continuous interactions with neighboring adipocytes, immune cells, ECs, and the ECM. Future studies integrating spatial, functional, and intercellular communication analyses will be essential to capture ASPCs as part of a dynamic tissue ecosystem rather than as discrete cell states. Such an integrated framework will be key to translating ASPC heterogeneity into mechanistic insight and therapeutic opportunity.

SUPPLEMENTARY MATERIALS

Supplementary materials related to this article can be found online at https://doi.org/10.4093/dmj.2025.1182.

CONFLICTS OF INTEREST

No potential conflict of interest relevant to this article was reported.

ORCID

Maxi Albert *https://orcid.org/0009-0008-1623-6823*
Lucas Massier *https://orcid.org/0000-0002-6199-2643*

FUNDING

This study was supported by a starting grant from the Swedish Research Council (VR), the Deutsche Forschungsgemeinschaft (DFG, German Research Foundation) under Germany's Excellence Strategy–EXC-3105/1–533765739, the German Diabetes Association (DDG) and the European Association for the Study of Diabetes (EASD).

ACKNOWLEDGMENTS

None

REFERENCES

1. Ouellet V, Labbe SM, Blondin DP, Phoenix S, Guerin B, Haman F, et al. Brown adipose tissue oxidative metabolism contributes to energy expenditure during acute cold exposure in humans. J Clin Invest 2012;122:545-52.
2. Bartesaghi S, Hallen S, Huang L, Svensson PA, Momo RA, Wallin S, et al. Thermogenic activity of UCP1 in human white fat-derived beige adipocytes. Mol Endocrinol 2015;29:130-9.
3. Emont MP, Jacobs C, Essene AL, Pant D, Tenen D, Colleluori G, et al. A single-cell atlas of human and mouse white adipose tissue. Nature 2022;603:926-33.
4. Vijay J, Gauthier MF, Biswell RL, Louiselle DA, Johnston JJ, Cheung WA, et al. Single-cell analysis of human adipose tissue identifies depot and disease specific cell types. Nat Metab 2020;2:97-109.
5. Raheem J, Sliz E, Shin J, Holmes MV, Pike GB, Richer L, et al. Visceral adiposity is associated with metabolic profiles predictive of type 2 diabetes and myocardial infarction. Commun Med (Lond) 2022;2:81.
6. Westcott GP, Emont MP, Li J, Jacobs C, Tsai L, Rosen ED. Mesothelial cells are not a source of adipocytes in mice. Cell Rep 2021;36:109388.
7. Hagberg CE, Spalding KL. White adipocyte dysfunction and obesity-associated pathologies in humans. Nat Rev Mol Cell Biol 2024;25:270-89.
8. Festa J, AlZaim I, Kalucka J. Adipose tissue endothelial cells: insights into their heterogeneity and functional diversity. Curr Opin Genet Dev 2023;81:102055.
9. Alzaid F, Fagherazzi G, Riveline JP, Bahman F, Al-Rashed F, Al-Mulla F, et al. Immune cell-adipose tissue crosstalk in metabolic diseases with a focus on type 1 diabetes. Diabetologia

2025;68:1616-31.
10. Sondergaard RH, Hojgaard LD, Reese-Petersen AL, Hoeeg C, Mathiasen AB, Haack-Sorensen M, et al. Adipose-derived stromal cells increase the formation of collagens through paracrine and juxtacrine mechanisms in a fibroblast co-culture model utilizing macromolecular crowding. Stem Cell Res Ther 2022;13:250.
11. Kohda H, Tanaka M, Shichino S, Arakawa S, Komori T, Ito A, et al. Novel cell-to-cell communications between macrophages and fibroblasts regulate obesity-induced adipose tissue fibrosis. Diabetes 2025;74:1135-52.
12. Hepler C, Shan B, Zhang Q, Henry GH, Shao M, Vishvanath L, et al. Identification of functionally distinct fibro-inflammatory and adipogenic stromal subpopulations in visceral adipose tissue of adult mice. Elife 2018;7:e39636.
13. Cattaneo P, Mukherjee D, Spinozzi S, Zhang L, Larcher V, Stallcup WB, et al. Parallel lineage-tracing studies establish fibroblasts as the prevailing in vivo adipocyte progenitor. Cell Rep 2020;30:571-82.
14. Zhang R, Gao Y, Zhao X, Gao M, Wu Y, Han Y, et al. FSP1-positive fibroblasts are adipogenic niche and regulate adipose homeostasis. PLoS Biol 2018;16:e2001493.
15. Uhrbom M, Muhl L, Genove G, Liu J, Palmgren H, Alexandersson I, et al. Adipose stem cells are sexually dimorphic cells with dual roles as preadipocytes and resident fibroblasts. Nat Commun 2024;15:7643.
16. Gu S, Gong Z, Liu S, Lu G, Ling Y, Wei Y, et al. Global single-cell sequencing landscape of adipose tissue of different anatomical site origin in humans. Stem Cells Int 2023;2023:8282961.
17. Angueira AR, Sakers AP, Holman CD, Cheng L, Arbocco MN, Shamsi F, et al. Defining the lineage of thermogenic perivascular adipose tissue. Nat Metab 2021;3:469-84.
18. Gupta RK, Arany Z, Seale P, Mepani RJ, Ye L, Conroe HM, et al. Transcriptional control of preadipocyte determination by Zfp423. Nature 2010;464:619-23.
19. He T, Wang S, Li S, Shen H, Hou L, Liu Y, et al. Suppression of preadipocyte determination by SOX4 limits white adipocyte hyperplasia in obesity. iScience 2023;26:106289.
20. Ferrero R, Rainer PY, Rumpler M, Russeil J, Zachara M, Pezoldt J, et al. A human omentum-specific mesothelial-like stromal population inhibits adipogenesis through IGFBP2 secretion. Cell Metab 2024;36:1566-85.e9.
21. Hildreth AD, Ma F, Wong YY, Sun R, Pellegrini M, O'Sullivan TE. Single-cell sequencing of human white adipose tissue identifies new cell states in health and obesity. Nat Immunol 2021;22:639-53.
22. Martinez-Colon GJ, Ratnasiri K, Chen H, Jiang S, Zanley E, Rustagi A, et al. SARS-CoV-2 infection drives an inflammatory response in human adipose tissue through infection of adipocytes and macrophages. Sci Transl Med 2022;14:eabm9151.
23. Reinisch I, Ghosh A, Noe F, Sun W, Dong H, Leary P, et al. Unveiling adipose populations linked to metabolic health in obesity. Cell Metab 2025;37:640-55.
24. Whytock KL, Divoux A, Sun Y, Pino MF, Yu G, Jin CA, et al. Aging human abdominal subcutaneous white adipose tissue at single cell resolution. Aging Cell 2024;23:e14287.
25. Divoux A, Whytock KL, Halasz L, Hopf ME, Sparks LM, Osborne TF, et al. Distinct subpopulations of human subcutaneous adipose tissue precursor cells revealed by single-cell RNA sequencing. Am J Physiol Cell Physiol 2024;326:C1248-61.
26. Koczkowska M, Kostecka A, Zawrzykraj M, Myszczynski K, Skoniecka A, Deptula M, et al. Identifying differentiation markers between dermal fibroblasts and adipose-derived mesenchymal stromal cells (AD-MSCs) in human visceral and subcutaneous tissues using single-cell transcriptomics. Stem Cell Res Ther 2025;16:64.
27. Garcia-Honduvilla N, Cifuentes A, Ortega MA, Delgado A, Gonzalez S, Bujan J, et al. High sensitivity of human adipose stem cells to differentiate into myofibroblasts in the presence of C. aspersa egg extract. Stem Cells Int 2017;2017:9142493.
28. Liu X, Yuan M, Xiang Q, Li Z, Xu F, Chen W, et al. Single-cell RNA sequencing of subcutaneous adipose tissues identifies therapeutic targets for cancer-associated lymphedema. Cell Discov 2022;8:58.
29. Palani NP, Horvath C, Timshel PN, Folkertsma P, Gronning AG, Henriksen TI, et al. Adipogenic and SWAT cells separate from a common progenitor in human brown and white adipose depots. Nat Metab 2023;5:996-1013.
30. Merrick D, Sakers A, Irgebay Z, Okada C, Calvert C, Morley MP, et al. Identification of a mesenchymal progenitor cell hierarchy in adipose tissue. Science 2019;364:eaav2501.
31. Bui HV, Hansen JK, Lo Sardo V, Galmozzi A. White and brown adipose tissue share a convergent fibro-adipogenic progenitor population. EMBO Rep 2025;26:5612-36.
32. Miranda AMA, McAllan L, Mazzei G, Andrew I, Davies I, Ertugrul M, et al. Selective remodelling of the adipose niche in obesity and weight loss. Nature 2025;644:769-79.
33. Sarvari AK, Van Hauwaert EL, Markussen LK, Gammelmark E, Marcher AB, Ebbesen MF, et al. Plasticity of epididymal ad-

ipose tissue in response to diet-induced obesity at single-nucleus resolution. Cell Metab 2021;33:437-53.
34. Massier L, Jalkanen J, Elmastas M, Zhong J, Wang T, Nono Nankam PA, et al. An integrated single cell and spatial transcriptomic map of human white adipose tissue. Nat Commun 2023;14:1438.
35. Garritson JD, Zhang J, Achenbach A, Ferhat M, Eich E, Stubben CJ, et al. BMPER is a marker of adipose progenitors and adipocytes and a positive modulator of adipogenesis. Commun Biol 2023;6:638.
36. Loft A, Emont MP, Weinstock A, Divoux A, Ghosh A, Wagner A, et al. Towards a consensus atlas of human and mouse adipose tissue at single-cell resolution. Nat Metab 2025;7:875-94.
37. Marcelin G, Da Cunha C, Gamblin C, Suffee N, Rouault C, Leclerc A, et al. Autophagy inhibition blunts PDGFRA adipose progenitors' cell-autonomous fibrogenic response to high-fat diet. Autophagy 2020;16:2156-66.
38. Raajendiran A, Ooi G, Bayliss J, O'Brien PE, Schittenhelm RB, Clark AK, et al. Identification of metabolically distinct adipocyte progenitor cells in human adipose tissues. Cell Rep 2019;27:1528-40.
39. Chen M, Kim S, Li L, Chattopadhyay S, Rando TA, Feldman BJ. Identification of an adipose tissue-resident pro-preadipocyte population. Cell Rep 2023;42:112440.
40. Borrelli MR, Patel RA, Adem S, Diaz Deleon NM, Shen AH, Sokol J, et al. The antifibrotic adipose-derived stromal cell: grafted fat enriched with CD74+ adipose-derived stromal cells reduces chronic radiation-induced skin fibrosis. Stem Cells Transl Med 2020;9:1401-13.
41. Lehmann GM, Woeller CF, Pollock SJ, O'Loughlin CW, Gupta S, Feldon SE, et al. Novel anti-adipogenic activity produced by human fibroblasts. Am J Physiol Cell Physiol 2010;299:C672-81.
42. Ma H, Li YN, Song L, Liu R, Li X, Shang Q, et al. Macrophages inhibit adipogenic differentiation of adipose tissue derived mesenchymal stem/stromal cells by producing pro-inflammatory cytokines. Cell Biosci 2020;10:88.
43. Lee SH, Garske KM, Arasu UT, Kar A, Miao Z, Alvarez M, et al. Single nucleus RNA-sequencing integrated into risk variant colocalization discovers 17 cell-type-specific abdominal obesity genes for metabolic dysfunction-associated steatotic liver disease. EBioMedicine 2024;106:105232.
44. Kar A, Alvarez M, Garske KM, Huang H, Lee SHT, Deal M, et al. Age-dependent genes in adipose stem and precursor cells affect regulation of fat cell differentiation and link aging to obesity via cellular and genetic interactions. Genome Med 2024;16:19.
45. Chen ZJ, Das SS, Kar A, Lee SH, Abuhanna KD, Alvarez M, et al. Single-cell DNA methylome and 3D genome atlas of human subcutaneous adipose tissue. Nat Genet 2025;57:2238-49.
46. Lazarescu O, Ziv-Agam M, Haim Y, Hekselman I, Jubran J, Shneyour A, et al. Human subcutaneous and visceral adipocyte atlases uncover classical and nonclassical adipocytes and depot-specific patterns. Nat Genet 2025;57:413-26.
47. Peters H, Potla P, Rockel JS, Tockovska T, Pastrello C, Jurisica I, et al. Cell and transcriptomic diversity of infrapatellar fat pad during knee osteoarthritis. Ann Rheum Dis 2025;84:351-67.
48. Ha CW, Martin A, Sepich-Poore GD, Shi B, Wang Y, Gouin K, et al. Translocation of viable gut microbiota to mesenteric adipose drives formation of creeping fat in humans. Cell 2020;183:666-83.
49. Backdahl J, Franzen L, Massier L, Li Q, Jalkanen J, Gao H, et al. Spatial mapping reveals human adipocyte subpopulations with distinct sensitivities to insulin. Cell Metab 2021;33:1869-82.
50. Wu F, Wu F, Zhou Q, Liu X, Fei J, Zhang D, et al. A CCL2+ DPP4+ subset of mesenchymal stem cells expedites aberrant formation of creeping fat in humans. Nat Commun 2023;14:5830.
51. Wang H, Du Y, Huang S, Sun X, Ye Y, Sun H, et al. Single-cell analysis reveals a subpopulation of adipose progenitor cells that impairs glucose homeostasis. Nat Commun 2024;15:4827.
52. Ruoss S, Nasamran CA, Ball ST, Chen JL, Halter KN, Bruno KA, et al. Comparative single-cell transcriptional and proteomic atlas of clinical-grade injectable mesenchymal source tissues. Sci Adv 2024;10:eadn2831.
53. Loft A, Rydbirk R, Klinggaard EG, Van Hauwaert EL, Wernberg CW, Moller AF, et al. Single-cell-resolved transcriptional dynamics of human subcutaneous adipose tissue during lifestyle- and bariatric surgery-induced weight loss. Nat Metab 2026;8:260-78.
54. Whytock KL, Sun Y, Divoux A, Yu G, Smith SR, Walsh MJ, et al. Single cell full-length transcriptome of human subcutaneous adipose tissue reveals unique and heterogeneous cell populations. iScience 2022;25:104772.
55. Gupta A, Shamsi F, Altemose N, Dorlhiac GF, Cypess AM, White AP, et al. Characterization of transcript enrichment and detection bias in single-nucleus RNA-seq for mapping of distinct human adipocyte lineages. Genome Res 2022;32:242-57.
56. Kumar T, Nee K, Wei R, He S, Nguyen QH, Bai S, et al. A spa-

tially resolved single-cell genomic atlas of the adult human breast. Nature 2023;620:181-91.
57. Lim HJ, Wang Y, Buzdin A, Li X. A practical guide for choosing an optimal spatial transcriptomics technology from seven major commercially available options. BMC Genomics 2025; 26:47.
58. Liu P, Li D, Zhang J, He M, Gao D, Wang Y, et al. Comparative three-dimensional genome architectures of adipose tissues provide insight into human-specific regulation of metabolic homeostasis. J Biol Chem 2023;299:104757.
59. Saeed S, la Cour Poulsen L, Visnovska T, Hoffmann A, Ghosh A, Wolfrum C, et al. Chromatin landscape in paired human visceral and subcutaneous adipose tissue and its impact on clinical variables in obesity. EBioMedicine 2025;114:105653.
60. Hinte LC, Castellano-Castillo D, Ghosh A, Melrose K, Gasser E, Noe F, et al. Adipose tissue retains an epigenetic memory of obesity after weight loss. Nature 2024;636:457-65.
61. Williams MD, Joglekar MV, Satoor SN, Wong W, Keramidaris E, Rixon A, et al. Epigenetic and transcriptome profiling identifies a population of visceral adipose-derived progenitor cells with the potential to differentiate into an endocrine pancreatic lineage. Cell Transplant 2019;28:89-104.
62. Long Q, Yuan Y, Ou Y, Li W, Yan Q, Zhang P, et al. Integrative single-cell RNA-seq and ATAC-seq analysis of the evolutionary trajectory features of adipose-derived stem cells induced into astrocytes. J Neurochem 2025;169:e16269.
63. Fu Z, Jiang S, Sun Y, Zheng S, Zong L, Li P. Cut&tag: a powerful epigenetic tool for chromatin profiling. Epigenetics 2024; 19:2293411.
64. Xiao Y, Jin W, Ju L, Fu J, Wang G, Yu M, et al. Tracking single-cell evolution using clock-like chromatin accessibility loci. Nat Biotechnol 2025;43:784-98.
65. Luecken MD, Theis FJ. Current best practices in single-cell RNA-seq analysis: a tutorial. Mol Syst Biol 2019;15:e8746.
66. Heumos L, Schaar AC, Lance C, Litinetskaya A, Drost F, Zappia L, et al. Best practices for single-cell analysis across modalities. Nat Rev Genet 2023;24:550-72.
67. Hao Y, Stuart T, Kowalski MH, Choudhary S, Hoffman P, Hartman A, et al. Dictionary learning for integrative, multimodal and scalable single-cell analysis. Nat Biotechnol 2024;42:293-304.
68. Korsunsky I, Millard N, Fan J, Slowikowski K, Zhang F, Wei K, et al. Fast, sensitive and accurate integration of single-cell data with Harmony. Nat Methods 2019;16:1289-96.
69. Luecken MD, Büttner M, Chaichoompu K, Danese A, Interlandi M, Mueller MF, et al. Benchmarking atlas-level data integration in single-cell genomics. Nat Methods 2022;19:41-50.
70. La Manno G, Soldatov R, Zeisel A, Braun E, Hochgerner H, Petukhov V, et al. RNA velocity of single cells. Nature 2018; 560:494-8.
71. Bergen V, Lange M, Peidli S, Wolf FA, Theis FJ. Generalizing RNA velocity to transient cell states through dynamical modeling. Nat Biotechnol 2020;38:1408-14.
72. Rivera-Gonzalez GC, Butka EG, Gonzalez CE, Kong W, Jindal K, Morris SA. Single-cell lineage tracing reveals hierarchy and mechanism of adipocyte precursor maturation. bioRxiv [Preprint] 2023 Jun 3. https://doi.org/10.1101/2023.06.01.543318.
73. Kalgudde Gopal S, Dai R, Stefanska AM, Ansari M, Zhao J, Ramesh P, et al. Wound infiltrating adipocytes are not myofibroblasts. Nat Commun 2023;14:3020.
74. Troule K, Petryszak R, Cakir B, Cranley J, Harasty A, Prete M, et al. CellPhoneDB v5: inferring cell-cell communication from single-cell multiomics data. Nat Protoc 2025;20:3412-40.
75. Jin S, Plikus MV, Nie Q. CellChat for systematic analysis of cell-cell communication from single-cell transcriptomics. Nat Protoc 2025;20:180-219.
76. Jalkanen J, Zhong J, Nono Nankam PA, Bhalla N, Elmastas M, Luo J, et al. Cytoarchitectural multi-depot profiling reveals immune-metabolic crosstalk in human colon-associated adipose tissue. Cell Metab 2026;38:419-33.E9.
77. Nguyen H, Nguyen H, Tran D, Draghici S, Nguyen T. Fourteen years of cellular deconvolution: methodology, applications, technical evaluation and outstanding challenges. Nucleic Acids Res 2024;52:4761-83.
78. Green H, Meuth M. An established pre-adipose cell line and its differentiation in culture. Cell 1974;3:127-33.
79. Sun DD, Li XQ, Liu YT, Ge MQ, Hou ZC. The application of duck embryonic fibroblasts CCL-141 as a cell model for adipogenesis. Animals (Basel) 2024;14:2973.
80. Shamsi F, Tseng YH. Protocols for generation of immortalized human brown and white preadipocyte cell lines. Methods Mol Biol 2017;1566:77-85.
81. Rodriguez AM, Pisani D, Dechesne CA, Turc-Carel C, Kurzenne JY, Wdziekonski B, et al. Transplantation of a multipotent cell population from human adipose tissue induces dystrophin expression in the immunocompetent mdx mouse. J Exp Med 2005;201:1397-405.
82. Ahfeldt T, Schinzel RT, Lee YK, Hendrickson D, Kaplan A, Lum DH, et al. Programming human pluripotent stem cells into white and brown adipocytes. Nat Cell Biol 2012;14:209-

19.
83. Alameda MT, Osorio MR, Hernandez JJ, Rodriguez I. Hierarchical micro-nano topographies to control Bacteria and mesenchymal stem cells biological responses. Sci Rep 2025;15:25405.
84. Tontonoz P, Hu E, Spiegelman BM. Stimulation of adipogenesis in fibroblasts by PPAR gamma 2, a lipid-activated transcription factor. Cell 1994;79:1147-56.
85. Mathur N, Severinsen MC, Jensen ME, Naver L, Schrolkamp M, Laye MJ, et al. Human visceral and subcutaneous adipose stem and progenitor cells retain depot-specific adipogenic properties during obesity. Front Cell Dev Biol 2022;10:983899.
86. Stefkovich M, Traynor S, Cheng L, Merrick D, Seale P. Dpp4+ interstitial progenitor cells contribute to basal and high fat diet-induced adipogenesis. Mol Metab 2021;54:101357.
87. Wang C, Yin S, Cen L, Liu Q, Liu W, Cao Y, et al. Differentiation of adipose-derived stem cells into contractile smooth muscle cells induced by transforming growth factor-beta1 and bone morphogenetic protein-4. Tissue Eng Part A 2010;16:1201-13.
88. Marcelin G, Ferreira A, Liu Y, Atlan M, Aron-Wisnewsky J, Pelloux V, et al. A PDGFRα-mediated switch toward CD9high adipocyte progenitors controls obesity-induced adipose tissue fibrosis. Cell Metab 2017;25:673-85.
89. Schwalie PC, Dong H, Zachara M, Russeil J, Alpern D, Akchiche N, et al. A stromal cell population that inhibits adipogenesis in mammalian fat depots. Nature 2018;559:103-8.
90. Hattori H, Masuoka K, Sato M, Ishihara M, Asazuma T, Takase B, et al. Bone formation using human adipose tissue-derived stromal cells and a biodegradable scaffold. J Biomed Mater Res B Appl Biomater 2006;76:230-9.
91. Jin XB, Sun YS, Zhang K, Wang J, Ju XD, Lou SQ. Neocartilage formation from predifferentiated human adipose derived stem cells in vivo. Acta Pharmacol Sin 2007;28:663-71.
92. Mandl M, Ritthammer H, Ejaz A, Wagner SA, Hatzmann FM, Baumgarten S, et al. CRISPR/Cas9-mediated gene knockout in human adipose stem/progenitor cells. Adipocyte 2020;9:626-35.
93. Kamble PG, Hetty S, Vranic M, Almby K, Castillejo-Lopez C, Abalo XM, et al. Proof-of-concept for CRISPR/Cas9 gene editing in human preadipocytes: deletion of FKBP5 and PPARG and effects on adipocyte differentiation and metabolism. Sci Rep 2020;10:10565.
94. Iwayama T, Steele C, Yao L, Dozmorov MG, Karamichos D, Wren JD, et al. PDGFRα signaling drives adipose tissue fibrosis by targeting progenitor cell plasticity. Genes Dev 2015;29:1106-19.
95. Chen B, Zhu X, Zhang D, Zhu Z, Ye Q, Guo J. Adipose-derived mesenchymal stem cells suppress fibroblast proliferation of hypertrophic scar through CCL5 and CXCL12. Arch Dermatol Res 2024;316:527.
96. Yang C, Zhang H, Zeng C, Tian C, Liu W, Chen Y, et al. Exosomes from adipose-derived stem cells restore fibroblast function and accelerate diabetic wound healing. Heliyon 2024;10:e22802.
97. Hodge JG, Decker HE, Robinson JL, Mellott AJ. Tissue-mimetic culture enhances mesenchymal stem cell secretome capacity to improve regenerative activity of keratinocytes and fibroblasts in vitro. Wound Repair Regen 2023;31:367-83.
98. Thelen K, Watts SW, Contreras GA. Adipogenic potential of perivascular adipose tissue preadipocytes is improved by coculture with primary adipocytes. Cytotechnology 2018;70:1435-45. https://doi.org/10.1007/s10616-018-0238-0.
99. Li X, Wang H, Xu W. HGF and bFGF secreted by adipose-derived mesenchymal stem cells revert the fibroblast phenotype caused by vocal fold injury in a rat model. J Voice 2022;36:622-9.
100. Smith RJ, Faroni A, Barrow JR, Soul J, Reid AJ. The angiogenic potential of CD271+ human adipose tissue-derived mesenchymal stem cells. Stem Cell Res Ther 2021;12:160.
101. Steiner D, Mutschall H, Winkler S, Horch RE, Arkudas A. The adipose-derived stem cell and endothelial cell coculture system-role of growth factors? Cells 2021;10:2074.
102. Ortiz-Virumbrales M, Menta R, Perez LM, Lucchesi O, Mancheno-Corvo P, Avivar-Valderas A, et al. Human adipose mesenchymal stem cells modulate myeloid cells toward an anti-inflammatory and reparative phenotype: role of IL-6 and PGE2. Stem Cell Res Ther 2020;11:462.
103. Lee P, Werner CD, Kebebew E, Celi FS. Functional thermogenic beige adipogenesis is inducible in human neck fat. Int J Obes (Lond) 2014;38:170-6.
104. Halbgebauer D, Dahlhaus M, Wabitsch M, Fischer-Posovszky P, Tews D. Browning capabilities of human primary adipose-derived stromal cells compared to SGBS cells. Sci Rep 2020;10:9632.
105. Wang Q, Sun N, Kunzke T, Buck A, Shen J, Prade VM, et al. A simple preparation step to remove excess liquid lipids in white adipose tissue enabling improved detection of metabolites via MALDI-FTICR imaging MS. Histochem Cell Biol 2022;157:595-605.

106. Haartmans MJ, Claes BS, Emanuel KS, Tuijthof GJ, Heeren RM, Emans PJ, et al. Sample preparation for lipid analysis of intra-articular adipose tissue by using matrix-assisted laser desorption/ionization imaging. Anal Biochem 2023;662: 115018.
107. Merfeld-Clauss S, Gollahalli N, March KL, Traktuev DO. Adipose tissue progenitor cells directly interact with endothelial cells to induce vascular network formation. Tissue Eng Part A 2010;16:2953-66.
108. Nessbach P, Schwarz S, Becke TD, Clausen-Schaumann H, Machens HG, Sudhop S. Angiogenic potential of co-cultured human umbilical vein endothelial cells and adipose stromal cells in customizable 3D engineered collagen sheets. J Funct Biomater 2022;13:107.
109. Hunyenyiwa T, Hendee K, Matus K, Kyi P, Mammoto T, Mammoto A. Obesity inhibits angiogenesis through TWIST1-SLIT2 signaling. Front Cell Dev Biol 2021;9:693410.
110. Taylor J, Sellin J, Kuerschner L, Krahl L, Majlesain Y, Forster I, et al. Generation of immune cell containing adipose organoids for in vitro analysis of immune metabolism. Sci Rep 2020;10: 21104.
111. Escudero M, Vaysse L, Eke G, Peyrou M, Villarroya F, Bonnel S, et al. Scalable generation of pre-vascularized and functional human beige adipose organoids. Adv Sci (Weinh) 2023;10: e2301499.
112. Ioannidou A, Alatar S, Schipper R, Baganha F, Ahlander M, Hornell A, et al. Hypertrophied human adipocyte spheroids as in vitro model of weight gain and adipose tissue dysfunction. J Physiol 2022;600:869-83.
113. Huang R, Yang J, Yan Y, Liu X, Yin X, Liu C, et al. Direct differentiation of human adult adipose tissue into multilineage functional organoids. Engineering 2025;53:286-300.
114. Liu X, Yang J, Yan Y, Li Q, Huang RL. Unleashing the potential of adipose organoids: a revolutionary approach to combat obesity-related metabolic diseases. Theranostics 2024;14:2075-98.
115. Rojas-Rodriguez R, Lujan-Hernandez J, Min SY, DeSouza T, Teebagy P, Desai A, et al. Generation of functional human adipose tissue in mice from primed progenitor cells. Tissue Eng Part A 2019;25:842-54.
116. Brizio M, Mancini M, Lora M, Joy S, Zhu S, Brilland B, et al. Cytokine priming enhances the antifibrotic effects of human adipose derived mesenchymal stromal cells conditioned medium. Stem Cell Res Ther 2024;15:329.
117. Li Y, Zhang H, Ibanez CF, Xie M. Characterization of subcutaneous and visceral de-differentiated fat cells. Mol Metab 2025; 93:102105.
118. Gao Z, Daquinag AC, Su F, Snyder B, Kolonin MG. PDGFRα/PDGFRβ signaling balance modulates progenitor cell differentiation into white and beige adipocytes. Development 2018; 145:dev155861.
119. Rinkevich Y, Walmsley GG, Hu MS, Maan ZN, Newman AM, Drukker M, et al. Skin fibrosis. Identification and isolation of a dermal lineage with intrinsic fibrogenic potential. Science 2015;348:aaa2151.
120. Shen H, Huang X, Zhao Y, Wu D, Xue K, Yao J, et al. The Hippo pathway links adipocyte plasticity to adipose tissue fibrosis. Nat Commun 2022;13:6030.
121. Liu MH, Li Y, Han L, Zhang YY, Wang D, Wang ZH, et al. Adipose-derived stem cells were impaired in restricting CD4+T cell proliferation and polarization in type 2 diabetic ApoE-/- mouse. Mol Immunol 2017;87:152-60.
122. Phuong NQ, Bilal M, Nawaz A, Anh LD, Memoona, Aslam MR, et al. Role of transforming growth factor-β1 in regulating adipocyte progenitors. Sci Rep 2025;15:941.
123. Yang Loureiro Z, Joyce S, DeSouza T, Solivan-Rivera J, Desai A, Skritakis P, et al. Wnt signaling preserves progenitor cell multipotency during adipose tissue development. Nat Metab 2023;5:1014-28.
124. Lin JZ, Rabhi N, Farmer SR. Myocardin-related transcription factor A promotes recruitment of ITGA5+ profibrotic progenitors during obesity-induced adipose tissue fibrosis. Cell Rep 2018;23:1977-87.
125. Zhu Y, Zhang X, Gu R, Liu X, Wang S, Xia D, et al. LAMA2 regulates the fate commitment of mesenchymal stem cells via hedgehog signaling. Stem Cell Res Ther 2020;11:135.
126. Potts CM, Yang X, Lynes MD, Malka K, Liaw L. Exploration of conserved human adipose subpopulations using targeted single-nuclei RNA sequencing data sets. J Am Heart Assoc 2025; 14:e038465.
127. Zhang Y, Hua M, Ma X, Li W, Cao Y, Han X, et al. Dipeptidyl peptidase-4 marks distinct subtypes of human adipose stromal/stem cells with different hepatocyte differentiation and immunoregulatory properties. Stem Cell Res Ther 2024;15:338.
128. Longo KA, Wright WS, Kang S, Gerin I, Chiang SH, Lucas PC, et al. Wnt10b inhibits development of white and brown adipose tissues. J Biol Chem 2004;279:35503-9.
129. Xie YY, Mo CL, Cai YH, Wang WJ, Hong XX, Zhang KK, et al. Pygo2 regulates adiposity and glucose homeostasis via β-Catenin-Axin2-GSK3β signaling pathway. Diabetes 2018;

67:2569-84.
130. Kanazawa A, Tsukada S, Sekine A, Tsunoda T, Takahashi A, Kashiwagi A, et al. Association of the gene encoding wingless-type mammary tumor virus integration-site family member 5B (WNT5B) with type 2 diabetes. Am J Hum Genet 2004;75:832-43.
131. Zhu XY, Klomjit N, Conley SM, Ostlie MM, Jordan KL, Lerman A, et al. Impaired immunomodulatory capacity in adipose tissue-derived mesenchymal stem/stromal cells isolated from obese patients. J Cell Mol Med 2021;25:9051-9.
132. Conley SM, Hickson LJ, Kellogg TA, McKenzie T, Heimbach JK, Taner T, et al. Human obesity induces dysfunction and early senescence in adipose tissue-derived mesenchymal stromal/stem cells. Front Cell Dev Biol 2020;8:197.
133. Kawagishi-Hotta M, Hasegawa S, Igarashi T, Date Y, Ishii Y, Inoue Y, et al. Increase of gremlin 2 with age in human adipose-derived stromal/stem cells and its inhibitory effect on adipogenesis. Regen Ther 2019;11:324-30.
134. Joffin N, Paschoal VA, Gliniak CM, Crewe C, Elnwasany A, Szweda LI, et al. Mitochondrial metabolism is a key regulator of the fibro-inflammatory and adipogenic stromal subpopulations in white adipose tissue. Cell Stem Cell 2021;28:702-17.
135. Loh NY, Neville MJ, Marinou K, Hardcastle SA, Fielding BA, Duncan EL, et al. LRP5 regulates human body fat distribution by modulating adipose progenitor biology in a dose- and depot-specific fashion. Cell Metab 2015;21:262-73.
136. Wang B, Fu X, Zhu MJ, Du M. Retinoic acid inhibits white adipogenesis by disrupting GADD45A-mediated Zfp423 DNA demethylation. J Mol Cell Biol 2017;9:338-49.
137. Guan L, Hu X, Liu L, Xing Y, Zhou Z, Liang X, et al. Bta-miR-23a involves in adipogenesis of progenitor cells derived from fetal bovine skeletal muscle. Sci Rep 2017;7:43716.
138. Spallanzani RG, Zemmour D, Xiao T, Jayewickreme T, Li C, Bryce PJ, et al. Distinct immunocyte-promoting and adipocyte-generating stromal components coordinate adipose tissue immune and metabolic tenors. Sci Immunol 2019;4:eaaw3658.
139. Buechler MB, Pradhan RN, Krishnamurty AT, Cox C, Calviello AK, Wang AW, et al. Cross-tissue organization of the fibroblast lineage. Nature 2021;593:575-9.
140. Spalding KL, Arner E, Westermark PO, Bernard S, Buchholz BA, Bergmann O, et al. Dynamics of fat cell turnover in humans. Nature 2008;453:783-7.
141. Harris CL, Pettigrew DM, Lea SM, Morgan BP. Decay-accelerating factor must bind both components of the complement alternative pathway C3 convertase to mediate efficient decay. J Immunol 2007;178:352-9.
142. Lee Y, Park YS, Choi NY, Kim YI, Koh YG. Proteomic analysis reveals commonly secreted proteins of mesenchymal stem cells derived from bone marrow, adipose tissue, and synovial membrane to show potential for cartilage regeneration in knee osteoarthritis. Stem Cells Int 2021;2021:6694299.
143. Abu-Shahba N, Mahmoud M, El-Erian AM, Husseiny MI, Nour-Eldeen G, Helwa I, et al. Impact of type 2 diabetes mellitus on the immunoregulatory characteristics of adipose tissue-derived mesenchymal stem cells. Int J Biochem Cell Biol 2021;140:106072.
144. Lu Z, Ding L, Zhang S, Jiang X, Ma W, Liu Y, et al. Adipose tissue-associated Krt23+fibroblasts contribute to immune microenvironment disorders in mouse adipose tissue during the development of obesity. Eur J Med Res 2025;30:708.
145. Zhong J, Zareifi D, Weinbrenner S, Hansen M, Klingelhuber F, Nono Nankam PA, et al. Adiposetissue.org: a knowledge portal integrating clinical and experimental data from human adipose tissue. Cell Metab 2025;37:566-9.
146. Goossens GH, Jocken JW, Blaak EE. Sexual dimorphism in cardiometabolic health: the role of adipose tissue, muscle and liver. Nat Rev Endocrinol 2021;17:47-66.
147. Mitterberger MC, Lechner S, Mattesich M, Zwerschke W. Adipogenic differentiation is impaired in replicative senescent human subcutaneous adipose-derived stromal/progenitor cells. J Gerontol A Biol Sci Med Sci 2014;69:13-24.
148. Choudhery MS, Badowski M, Muise A, Pierce J, Harris DT. Donor age negatively impacts adipose tissue-derived mesenchymal stem cell expansion and differentiation. J Transl Med 2014;12:8.
149. Maredziak M, Marycz K, Tomaszewski KA, Kornicka K, Henry BM. The influence of aging on the regenerative potential of human adipose derived mesenchymal stem cells. Stem Cells Int 2016;2016:2152435.

Supplementary Table 1. ASPC heterogeneity across recent single-cell and single-nuclei studies stratified by adipose depot: SAT, VAT, and other depots

Study	Method	Sample (*n*)	ASPC clusters	Characteristics of ASPC clusters
SAT				
Merrick et al. (2019) [29]	sc	ov/ob (8)	3 PDGFRA$^+$, PDGFRB$^+$, SCA1$^+$	(1) IP: DPP4, CD55, PI16, WNT2 (2) CPA: ICAM1, PPARG, GGT5, APOE, VCAM1, DEPP1 (3) SMC-like: ACTA2, THY1, APOE
Vijay et al. (2020) [4]	sc	ob (16): T2DM (6), non-T2DM (10)	7 CD34$^+$	(SP1) less mature PreAd/ASC: MGP, APOD, CXCL14, WISP2 (SP2) more mature PreAd: APOE, FABP4, CEBPB, CD36 (SP3) less mature PreAd/ASC: MGP, APOD, CXCL14, WISP2 (SP4) Fibro: FBN1, PI16, IGFBP6, COL3A1, COL6A3, COL1A1 (SP5) Inflammatory/HSC: CCL5, CD3E, IL7R, IL32, PTPRC
Backdahl et al. (2021) [49]	STx	le (3) ov (2) ob (5)	4 PDGFRA$^+$	(C07) PreAd/ASC: DCN, CXCL14, APOD, MGP (C09) UMP/Fibro: DCN, PRG4, FBN1, TNXP, VCAN, DPP4, CD55, PI16, CREB5 (C11) MTX: MT2A, MT1A, SOD2, MT1X, ADIRF, FABP4 (C12) mix of C07/C09: DCN, COL1A1, COL1A2, CFD, THY1, PI16, CFH, MGP, LPL
Hildreth et al. (2021) [21]	sc	le (3) ob (3)	3 ITGB1$^+$, PDGFRA$^+$, PDGFRB$^+$	(1) APC: PI16, DKK1, PRG4, DPP4 (2) PreAd: CD34, ICAM1, CXCL14, GPC3, APOD (3) IP (DPP4$^+$ PreAd-subtype): CD34, ICAM1, CD26, DPP4
Emont et al. (2022) [3]	sc, sn	sc: le (3), ov (4), ob (2) sn: le (2), ov (2), ob (9)	6 PDGFRA$^+$	(hASPC1): CEBPD, CXCL14, APOD, CXCL12, GPC3 (hASPC2) ASC: ALDH1A3, PRG4, FBN1, PI16, CD55, DPP4, COL1A1 (hASPC3): FGF10, C7, FMO2, PRKG11, ABCA10 (hASPC4) Areg: EPHA3, F3, KCNIP1, PTCH2, FLRT2, SLIT2 (hASPC5): SGCZ, PDZRN4, PIEZO2, NOX4, TWIST1 (hASPC6): PDE4D, CLIC5, GLI3, WT1
Martinez-Colon et al. (2022) [22]	sc	ob (3)	11 CD34$^+$	(C0) PreAd: IL11, PTGS2 (C3) PreAd: MMP3, MMP1 (C4, P15)[a] PreAd/Inflammatory: COL3A1, DCN, IGF1, ISG15, COL1A2, COL6A3 (C5) PreAd: HIST1H4C, HIST1H1A (C7) PreAd: PTX3, ADM (C10) PreAd: SNHG15, IL1R1 (C11) PreAd: UBE2C, TOP2A (C13) PreAd: HSPA6, HSPA1A (C14) PreAd: NEAT1, MTRNR2L8(C15) PreAd: CCL20, PTGS2 (C16, P9) PreAd/ASC: MGP, CFD, CXCL14, APOD
Liu et al. (2022) [28]	sc	ly (5): ov (5) Non-ly (4): le (2), ov (2)	4 PDGFRA$^+$, DCN$^+$, CD34$^+$, CD105$^+$, CD73$^+$, THY1$^+$, CD59$^+$, CD44$^+$, ITGB1$^+$, CSF1$^+$	(c0) CPA: GGT5, CXCL14, APOD, APOE, MGP, WISP2, C7, (c1) transient IP>CPA state: CD9, MMP2, POSTN, WISP2, COL14A1, CTHRC1, DPP4 (c3) IP: DPP4, CD55, PRG4, FBN1, LOXL1, EFHD1, CLEC3B (c5) MTX/stress-responsive: CHI3L1, HLA-DRA, HLA-DRB1, HLA-DRB5, MT1X, MT2A, MT1E, MT1G, MT1M, MT1A
Whytock et al. (2022) [54]	sc, sn[b] full-length (SMARTseq)	ov (1) ob (1)	5 (sc), 4 (sn) No general marker Stem (sc: 3, sn: 1) CD34$^+$, PDGFRA$^+$, PDGFRB$^+$ PreAd (sc: 2, sn: 3) ATXN1$^+$, ZNF423$^+$, CD38$^+$	sc (Stem 1): DCN, PDGFRA, CXCL14, FBN1, APOD, FMO1 (Stem 2): DCN, PDGFRA, PDGFRB, CD34, THY1, CFD, PRG4, COL1A1 (Stem 3): PDGFRB, ABCA10, CXCL14, FBLN1, APOD, MGP, MMP2, COL6A3 (PreAd 1): ATXN1, ZNF423RBFOX1, DZX4, CSMD1 (PreAd 2): CD38, DLK1, DGAT2, GPT2, PLCH2 sn (Stem) PDGFRA, CD34, DCN, COL1A1, COL1A2, CXCL14 (PreAd 1) ZNF423, HDC, HPGD, BTK (PreAd 2) ATXN1, ZNF274, lncRNA562, SLC16A5 (PreAd 3) CD38, FAM13C, HBA2, PDE9A

(*Continued to the next page*)

Supplementary Table 1. Continued

Study	Method	Sample (*n*)	ASPC clusters	Characteristics of ASPC clusters
Gu et al. (2023) [16]	sc	(1)Σ13	12 No general marker Fibro (1)$^{+}$ASC (3) ENG^{+}, MME^{+}, FAP^{+} PreAd (8) APOD^{+}, CXCL14^{+}, MGP^{+}	(1) Fibro: TXNIP (2) ASC: SDC1 (3) ASC: APOD (4) ASC: IGFBP5 (5) PreAd: APOE (6) PreAd: DEPP1 (7) PreAd: PDGFRL (8) PreAd: DSP (9) PreAd: TPPP3 (10) PreAd: TK1 (11) PreAd: CIAO2A (12) PreAd: RAI14
Massier et al. (2023) [34]	sc, sn, STx	le (3) ov (1) ob (9) Σ83	17 CD34^{+}, PDGFRA^{+}, PDGFRB^{+}	(sfC0) CPA: APOD, CXCL14, CFD (sfC01) FAP: NEGR1, EBF1, ABCA10 (sfC02) APC: PI16, CD55, COL1A1, COL1A2 (sfC03) CD34^{-} FAP: CALN1. COL19A1, DLGAP1 (sfC04) FAP: APOD, CXCL14, TXNIP (sfC05) FAP/MTX: MT2A, MT1X, TIMP1 (sfC06) FAP: SEMA3C, ROBO2, EBF1 (sfC07) FAP: COL3A1, COL1A1, COL1A2 (sfC08) FAP: TPT1, MGP, APOD (sfC09) FAP: ABCA8, ABCA9, ABCA10, RORA (sfC10) FAP: FBN1, EBF2, ADAMTSL1 (sfC11) MSL: ITLN1, MSLN, EZR (sfC12) FAP: ABCA10, SLIT2, LAMA2 (sfC13) FAP: CD74, HLA-DRA, FABP4 (sfC14) FAP: PTPRG, COL4A1, COL4A2 (sfC15) FAP: SLC4A7, ACSL4 (sfC16) late CPA: PLIN1, PDE3B, PPARG
Divoux et al. (2024) [25]	sc	ov/ob (8) ABD-/GF-SAT, apple- vs. pear-shaped women	6 DCN^{+}, PDGFRA^{+}, PDGFRB^{+}	(CPA 1) ZNF423, CD38, DLK1, PPARG, LOX, MFAP5 (CPA 2) ZNF423, CD38, MFAP5 (MSC 1) VIM, PDGFRB (MSC 2) DPP4, CD55, CD44, THY1, POSTN, VIM (MSC 3) DPP4, THY1, LUM (SMC-like) ITGA5, CD55, CD44, THY1, MYL9, ACTA2
Ferrero et al. (2024) [20]	sc	ob (3)	6 TM4SF1^{-}, Lin^{-} (CD45, PECAM1)	(1) ASC: DPP4, CD55, PI16, PRG4, LY6A, CD24 (2) PreAd: ICAM1, PPARG, PDGFRA, FABP4, APOC, APOD (3) HHIP^{+}/Areg^{c}: IGFBP7, NOV, ALDH1A1, EPHA3, APOD, SLIT2, MGP, F3 (4) IFIT^{+}: ISG15, IFI6, IFI27, MX1, MX2 (5) SFRP4^{+}: SFRP2, CTHRC1, COL14A1, WSP2, MGP (6) RBP5^{+}: COL3A1, COL6A1, COL6A3, APOE
Ruoss et al. (2024) [52]	sc	le (4) ov (4) ob (3)	11 No general marker Prefibrocytes (3) MSR1, ITGAX, FBP1, SPP1 Fibro(7) DCN^{+}, CFD^{+}, PDGFRA^{+} Early PreAds (1) PLIN1^{+}, CIDEA^{+}, CIDEC^{+}, ADIPOQ^{+}	(1) Prefibrocytes (early): RGS5, APOLD1, RBP7, CD52, MSR1, KDR, CDH5, ITGA6 (2) Prefibrocytes (late): TNXB, CFD, MGP, COL6A2, CD55, LRP1, CD44, CD74, IL7R (3) early Fibro/Fibrocytes: CD34, PTPRC, CD14, CD68, CD163 (4, P1) Fibro: CXCL14, APOD, APOE, CXCL12, SLC15A3, VCAM1, CD36 (5, P2) Fibro: CILP, ITGA11, ANGPTL2, PLA2Ga, KLF6 (6, P3) C1QTNF3^{+}-Fibro/UMP: PRG4, CD55, DPP4, FBN1, SFRP4, SEMA3C, CD70 (7, P4) Fibro/IPA/MTX: ICAM1, PDGFRB, CD36, CCL2, POSTN, MT1X, MT2A (8, P5) hedgehog-Fibro: HHIP, PTCH2, IGFBP7, BGN, NRP1, F3 (9, P6) COL8A1^{+}-Fibro: COMP, PCSK5, MGP, SFRP2, F3 (10, P7) dendritic-like Fibro: CD74, C1QA, HLA-DRA, CCL3, CD36, MRC1 (11) early PreAd: PLIN1, ADIPOQ, PLIN4, RBP4, SAA1, G0S2, CD36, MCAM

(*Continued to the next page*)

Supplementary Table 1. Continued

Study	Method	Sample (*n*)	ASPC clusters	Characteristics of ASPC clusters
Whytock et al. (2024) [24]	sn full-length (SMARTseq)	20–30 years: le (4); ov (3), ob (3) 65–89 years: le (1), ov (5), ob (5)	2 No general marker	(Stem): PDGFRA, DCN, C3, LUM, APOD, CXCL14, MGP, COL1A1 COL1A2, COL3A1, COL6A3 (PreAd): ZNF423, RBFOX1, PTPRD, CTNNA2, NRXN3, CNTNAP2
Lazarescu et al. (2025) [46]	sn	ob (5)	5 PDGFRA^{+} (except for cluster 4)	(1) ASC: DPP4, CD55 (2) CPA: PPARG (3) DPP4, CD55, CD9, THY1, ITGB1, CD55 (4) PDE4D (5) ALDH1A3, CD55
Loft et al. (2026) [53]	sn	ob (14)[d]	4 PDGFRA^{+}, DCN^{+}	(1) UMP/IP: DPP4, SEMA3C, FBN1 (2) committed ASPCs: CXCL14, CFD, C3 (3) PreAd: PPARG, ACACB, CD36, SEMA3A (4) Areg: EPHA3, F3, MEOX2, IGFBP7
Miranda et al. (2025) [32]	sn, STx	le (24) ob (25)[e]	5 No general marker	(APC1/ASC) UMP: DCN, DPP4, CD55, ITGA11 (APC2) CPA: PPARG, GPC3, COL15A1 (APC3) CPA (stressed): PDGFRA, PPARG, GPC3, JUN, FOSB (APC4) Areg[f]: PDGFRA, KCNIP1, F3, EPHA3, GPC3 (APC5) Profibrotic: PDGFRA, PPARG, ADAM12, POSTN, VCAN, HIF1A
Reinisch et al. (2025) [23]	sn	ob (77): MHO (32), MUO (45)	4 PDGFRA^{+}, LAMA2^{+}	(1) UMP[g]: PI16, DPP4, CD55, CD34, MFAP5 (2) Areg[g]: EPHA3, SEMA5A, BOC, F3 (3) CPA1: FMO2, CD36, PPARG, LMO3, BOC (4) CPA2: ICAM1, LDLR, MEDAG, CTSL
VAT				
Vijay et al. (2020) [4]	sc	ob (16) subtypes: T2DM (6), non-T2DM (10)	6 CD34^{+} (VP1-3) MSLN^{+}, WT1^{+}, UPK3B^{+} (VP4-6) CFD^{+}	(VP1): UCP1, PLA2G2A, SLPI, MT-ND5, PRG4 (VP2): SLPI, RPS26, TPM2 (VP3): SOD2, CCL2, NAMPT, KRT8, KRT18, MT1A, MT2A, PRG4 (VP4) less mature PreAd/ASC: MGP, APOD, CXCL14, GPX3, EIF1, MT1A (VP5) Fibro: MFAP5, S100A4 (VP6) Inflammatory/HSC: TYROBP, HLA-DRA, CD74
Emont et al. (2022) [3]	sn	le (2) ov (1) ob (7)	6 PDGFRA^{+}	(hASPC1): CEBPD, CXCL14, APOD, CXCL12, GPC3 (hASPC2) ASC: ALDH1A3, PRG4, FBN1, PI16, CD55, DPP4, COL1A1 (hASPC3): FGF10, C7, FMO2, PRKG11, ABCA10 (hASPC4) Areg: EPHA3, F3, KCNIP1, PTCH2, FLRT2, SLIT2 (hASPC5): SGCZ, PDZRN4, PIEZO2, NOX4, TWIST1 (hASPC6): PDE4D, CLIC5, GLI3, WT1
Martinez-Colon et al. (2022) [22]	sc	ob (3)	13 CD34^{+}	(C0) PreAd: IL11, PTGS2 (C1, P1/4)[a]: PreAd/MSL: KRT18, ALDH1A3, MSLN (C3): PreAd: MMP3, MMP1 (C4) PreAd: COL3A1, DCN, KRT18, MSLN (C5) PreAd: HIST1H4C, HIST1H1A (C7) PreAd: PTX3, ADM (C9, P1/4)[a] PreAd/MSL: SLPI, KRT8 (C10) PreAd: SNHG15, IL1R1 (C13) PreAd: HSPA6, HSPA1A (C14) PreAd: NEAT1, MTRNR2L8 (C15) PreAd: CCL20, PTGS2 (C16, P9)[a] PreAd/ASC: MGP, CFD, CXCL14, APOD (C22, P1/4)[a] PreAd/MSL: SLPI, KRT8

(*Continued to the next page*)

Supplementary Table 1. Continued

Study	Method	Sample (*n*)	ASPC clusters	Characteristics of ASPC clusters
Garritson et al. (2023) [35]	sc	le (4) ob (5)	4 (8)[h] PDGFRA$^+$	(FAP1) PreAd: FMO2, IGFBP3, PTGDS, CXCL12, CXCL14, APOD, TXNIP (FAP2) Inflammatory/stress-responsive: MT1A, CCL2, NAMPT, THBS1, MT1X, PTX3, SOD2, MT1M, CXCL2, NNMT, MT2A (FAP3) UMP/stem-like: SEMA3C, SLPI, MFAP5, PI16, CD55, PRG4, IFI27, FBN1, PLA2G2A, VCAN, HTRA3 (FAP4) Fibro-progenitor/Areg: SFRP4, CD9, COL14A1, CTHRC1, THY1, IGFBP2, COL1A1, WISP2, APOE Higher-resolution subclustering analysis[h]: (0) CPA: APOD, CXCL14 (1) UMP[i]: PI16[n], SEMA3C[n], OSR2[n], CD55, PRG4 (2) Areg[j]: THY1, CTHRC1 (3) immune cell-like: PTX3, CCL2, MT1A, MT1X (4) committed APC: ICAM1[n], CEBPB[n] (5) CPA: APOD, CXCL14 (6) Profibrotic/Fibro-progenitors: VCAN[n], MFAP5[n], HTRA3[n] (7) immune cell-like: PTX3, CCL2, MT1A, MT1X
Gu et al. (2023) [16]	sc	(1)Σ12	8 No general marker Fibro (1)$^+$ASC (1) ENG$^+$, MME$^+$, FAP$^+$ PreAd (6) APOD$^+$, CXCL14$^+$, MGP$^+$	(1) Fibro: TXNIP (2) ASC: APOD (3) PreAd: ITLN1 (4) PreAd: DSP (5) PreAd: TK1 (6) PreAd: CIAO2A (7) PreAd: RAI14 (8) PreAd: PTGDS
Massier et al. (2023) [34]	sc, sn, STx	ob (5)Σ83	15 CD34$^+$, PDGFRA$^+$, PDGFRB$^+$	(ofC0) FAP: ADIRF, TMSB4X, TPT1 (ofC01) FAP: KRT18, MT2A, TIMP1 (ofC02) CPA: APOD, CFD (ofC03) MSL: DPP4, EZR, PLCB1 (ofC04) FAP: CLIC4, CUX1, SAMD4A (ofC05) FAP: NEGR1, ABCA10, ABCA9 (ofC06) MSL: DPP4, EZR, ERBB4 (ofC07) APC: CD55, PI16 (ofC08) FAP: CRISPLD2, ZNF331 (ofC09) FAP: NOVA1, EBF1, FBN1 (ofC10) FAP: CD74, FTL, FTH1 (ofC11) MSL: DPP4, LRP2 (ofC12) MSL: PKHD1L1, ZBTB16 (ofC13) PDGFRB$^-$ FAP: CNTNAP2, CSMD1 (ofC14) FAP: LAMA2, FKBP5, PTPRG
Ferrero et al. (2024) [20]	sc	ob (3)	7 TM4SF1$^-$, Lin$^-$ (CD45, PECAM1) (IGFBP2$^+$: TM4SF1$^+$)	(1) ASC: DPP4, CD55, PI16, PRG4, LY6A, CD24 (2) PreAd: ICAM1, PPARG, PDGFRA, FABP4, APOC, APOD (3) HHIP$^+$/Areg[c]: IGFBP7, NOV, ALDH1A1, EPHA3, APOD, SLIT2, MGP, F3 (4) IFIT$^+$: ISG15, IFI6, IFI27, MX1, MX2 (5) SFRP4$^+$: SFRP2, CTHRC1, COL14A1, WSP2, MGP (6) RBP5$^+$: COL3A1, COL6A1, COL6A3, APOE (7) IGFBP2^{+c}: G0S2, C7, RBP1
Wang et al. (2024) [51]	sc	le (2) ob (6): non-T2DM (3), T2DM (3)	4 PDGFRA$^+$, APOD$^+$, CD34$^+$, THY1$^+$	(1) UMP: CD55, PI16, SLPI, SEMA3C (2) CD9, COL14A1, RARRES1, SFRP4 (3) CPA: ICAM1, NABP1, ABHD5, ATF3 (4) Areg: F3, SVEP1, ABCA8, CXCL12
Lazarescu et al. (2025) [46]	sn	le (1) ov (1) ob (7) NA (1)	4 PDGFRA$^+$	(1) CD55, ALDH1A3 (2) PPARG, F3 (3) ITGB1, THY1, F3 (4) PDE4D, ALDH1A3, WT1

(*Continued to the next page*)

Supplementary Table 1. Continued

Study	Method	Sample (*n*)	ASPC clusters	Characteristics of ASPC clusters
Reinisch et al. (2025) [23]	sn	MHO (32) MUO (45)	5 PDGFRA^{+}, LAMA2^{+}	(1) UMP^{g}: PI16, DPP4, CD55, CD34, MFAP5 FAPs (2) Areg1^{g}: EPHA3, CD36, BOC, F3 (3) Areg2^{g}: EPHA3, ZNF804B, CCL12, IL15, SEMA5A (4) CPA1: FMO2, BOC, F3 (5) CPA2: ICAM1, LDLR, MEDAG, CTSL
Other depots				
Ha et al. (2020) [48]	sc	CD (11) UC (13) Creeping fat, mesenteric AT	5 No general marker	(P1) SFRP2, MGP, DCN, WISP2, COL1A1, COL3A1, COL6A3 (P2) CD34, FABP4, PPARG, SEMA3C, POSTN, FBN1 (P3) FABP4, CFD, PLA2G2A, CXCL12, GPC3, GPX3, PDGFRA, APOD (P4) ICAM1, DEPP1, FMO2, SVEP1, APOD (P5) TPX2, BIRC5, TOP2A, TYMS
Angueira et al. (2021) [17]	sn	le (1) ov (1) ob (1) Aortic PVAT	5 Lin^{-} (CD45, PECAM1, CD235a)	(1) Fibro/Progenitor: PDGFRA, CD55, PI16, MFAP5, LY6A (2) Intermediate/Transitional: F3, CD200, PPARG, PDGFRA (3) PreAd-1: PPARG, PDGFRA, COL15A1 (4) PreAd-2: PPARG, PDGFRA, COL4A4, FOSB (5) SMC-like: PPARG, PDGFRB, SEMA5A, TRPC6, NOTCH3, MCAM
Gu et al. (2023) [16]	sc	(1)∑3 Subcutaneous leg AT^{k}	20 no general marker Fibro (6)$^{+}$ASC (10) ENG^{+}, MME^{+}, FAP^{+} PreAd (4) APOD^{+}, CXCL14^{+}, MGP^{+}	(1) Fibro: BIRC5 (2) Fibro: FBXO32 (3) Fibro: TK1 (4) Fibro: TXNIP (5) Fibro: LSP1 (6) Fibro: OSMR (7) ASC: SDC1 (8) ASC: PAPPA (9) ASC: APOD (10) ASC: TOP2A (11) ASC: ACAN (12) ASC: CFD (13) ASC: G0S2 (14) ASC: IGFBP5 (15) ASC: H19 (16) ASC: KRT19 (17) PreAd: CIAO2A (18) PreAd: DSP (19) PreAd: DEPP1 (20) PreAd: APOE
Kumar et al. (2023) [56]	sc	le (16) ov (33) ob (71) un (1) NA (5)^{l} Breast AT	4 GLI2^{+}, HMGA2^{+}, WISP2^{+}, PLAGL^{+}	(1) Fibro-major: MMP3, CXCL1, CXCL2, CXCL3, CEBPB, THS1 (2) Fibro-matrix: COL1A1, COL3A1, COL15A1, POSTN, IGF1, TNC (3) Fibro-prematrix: GPX3, WISP2, CXCL14, CFD, FOS, PLA-2G2A, C3, TXNIP (4) Fibro-SFRP4: SFRP4, MGP, G0S2, OGN, ADIRF, CD9, PRG4, COL14A1
Massier et al. (2023) [34]	sc, sn, STx	(0)∑3 PVAT	8 CD34^{+}, PDGFRA^{+}, PDGFRB^{+}	(pfC0) APC: CD55, PI16, PKHD1L1, EZR, ARHGAP44 (pfC01) FAP: FBLN1, KCND2, ABCA10, FBN1, COL6A3, COL15A1 (pfC02) FAP: PDE3B, ARL17B, C7, COL15A1, FMO2, CD36 (pfC03) CPA: APOD, CFD, KRT19, PRG4, TM4SF1, ABCA10, EZR (pfC04) FAP: SEMA3A, PLEKHG2, NAMPT, ABCA10, LAMA2, FOSB, FBLN1 (pfC05) FAP: SDK1, KCNB2, CNTN4, FBN1, COL5A1 (pfC06) FAP: CD55, FHOD3, MFAP5, FBN1, HN1, COL12A1, VCAN (pfC07) FAP: CEMIP, VEGFC, ADAMTS9, SEMA5A, RBFOX1, JUN, SVEP1

(*Continued to the next page*)

Supplementary Table 1. Continued

Study	Method	Sample (*n*)	ASPC clusters	Characteristics of ASPC clusters
Wu et al. (2023) [50]	sc	ob (1) ov (1) CD (9) Mesenteric AT	3 PDGFRA^{+}, THY1^{+}	(1) MSC1: DPP4, BMP8B (2) MSC2: F3, SFRP4 (3) MSC3: APOE, ICAM1, PPARG, FABP4
Ferrero et al. (2024) [20]	sc	ob (1) Mesocolic AT le (2) ov (1) Perirenal AT	7 TM4SF1^{-}, Lin^{-} (CD45, PECAM1)	for both, mesocolic and perirenal AT: (1) ASC: DPP4, CD55, PI16, PRG4, LY6A, CD24 (2) PreAd: ICAM1, PPARG, PDGFRA, FABP4, APOC, APOD (3) HHIP^{+}/Areg^{c}: IGFBP7, NOV, ALDH1A1, EPHA3, APOD, SLIT2, MGP, F3 (4) IFIT^{+}: ISG15, IFI6, IFI27, MX1, MX2 (5) SFRP4^{+}: SFRP2, CTHRC1, COL14A1, WSP2, MGP (6) RBP5^{+}: COL3A1, COL6A1, COL6A3, APOE (7) FMO2^{+m}: LMO3, MT-RNR1, MT-RNR2, ABCA6
Peters et al. (2025) [47]	sn	Non-OA (6) OA (15): le (7), ob (8) Infrapatellar fat pat (IFP)	5 PDGFRA^{+} (reduced in cluster 4)	(0) DPP4, PI16, CD34, FBN1, CD26, PIEZO2 (1) COL15A1, APOD, ABCA10, CD34, CD10 (2) CRTAC1, HLA-C, PRG4, FN1, SEMA3A (3) FABP4, ITGB8, ITGBL1, F13A1 (4) ENAH, MGAT4C, DCN, IGF1, COL14A1

Identified ASPC subclusters are listed according to the given names in the study, although our nomenclature suggests different names, revise foot notes for specific comments. Meta analysis are denoted as '(x)Σy,' where x represents the number of newly included patients in the study, and y indicates the number of previously published datasets incorporated into the analyses. Alternative gene names: ITGAX (CD11c), DPP4 (CD26), ITGB1 (CD29), ITGA6 (CD49f), ICAM1 (CD54), THY1 (CD90), LRP1 (CD91), VCAM1 (CD106), IL7R (CD127), PDGFRB (CD140b), F3 (CD142), CDH5 (CD144), MSR1 (CD204), NRP1 (CD304), KDR (CD309).

ASPC, adipose stromal and progenitor cell; SAT, subcutaneous adipose tissue; VAT, visceral adipose tissue; sc, single-cell RNA-sequencing; ov/ob, overweight or obese (body mass index [BMI] ≥25); IP, interstitial progenitor; CPA, committed preadipocyte; SMC, smooth muscle cell; ob, obese (BMI ≥30); T2DM, type 2 diabetes mellitus; SP, SAT progenitors (as defined in the referenced publication, Vijay et al.); Fibro, fibroblast-like; PreAd, pre-mature adipocyte; ASC, adipose stem cell; STx, spatial transcriptomic; le, lean (18.5≤ BMI <25); ov, overweight (25≤ BMI <30); UMP, uncommitted, multipotent progenitor cell; APC, adipose precursor cell; sn, single-nuclei RNA-sequencing; ly, stage III lymphedema; FAP, fibro-adipogenic progenitor; SMARTseq, Switching Mechanism At the 5′ end of the RNA Transcript sequencing; ABD, abdominal SAT; GF, gluteofemoral SAT; MSC/MSL, mesothelial cell; Lin, lineage (i.e., CD45^{-}, PECAM1^{-} cells=non-immune, non-endothelial); MHO, metabolically healthy obesity; MUO, metabolically unhealthy obesity; VP, VAT progenitor, as defined by the referenced publication (Vijay et al.); NA, unknown BMI or health status; CD, Crohn's disease; UC, ulcerative colitis; AT, adipose tissue; PVAT, perivascular adipose tissue; un, underweight (BMI <18.5); OA, osteoarthritis.

[a]Clusters 'C0–C22' were identified in the first annotation (Fig. 4A). Assigned cell types were used from Fig. 6 onwards (i.e., 'Adipose progenitors' as 'P0–P16'), but, to our understanding, no clear assignment was demonstrated. We assumed the matching C- and P-cluster according to the identified markers in the text and the dataset (Supplementary Data file S2) and the depot-specific abundances of C0-C22 (Supplementary Fig. S9D). The authors claim, that, i.e., P15 (Inflammatory ASPC) reacted to severe acute respiratory syndrome coronavirus-2 (SARS-CoV-2) infection in SAT.

[b]Whytock et al. [54] compared single-cell RNA-sequencing (scRNAseq) and single-nuclei RNA-sequencing (snRNAseq) and defined different clusters with both methods. ASPCs were divided into 'Stem and Pre-Ad' clusters, which had specific marker genes being differentially expressed in the subclusters, as shown in Figs. 1B (sn) and 3B (sc). Further, no general marker for ASPCs has been utilized.

[c]The authors discussed, whether the previously described Areg cluster is covered by either (3) HHIP^{+} or (7) IGFBP2^{+}. As the IGFBP2 population was only found in VAT and HHIP^{+} cells show a similar transcriptional pattern like the described EPHA3^{+} cluster [3], Aregs are associated with the HHIP^{+} subpopulation.

[d]Patients were enrolled for a bariatric surgery to the ATLAS study. Abdominal SAT biopsies were sampled after lifestyle-induced weight loss (WL) (5%–10%) and subsequent bariatric surgery-induced WL (20%–45%).

[e]This study included ob-samples before and after WL.

[f]The authors declared this cluster as 'adipogenesis-regulatory cells,' following our nomenclature, we name this subset Areg.

[g]The authors named clusters differently from our understanding of ASPC heterogeneity. Cluster (1) was names 'FAP,' but the characteristic marker genes most likely refer to UMP. Cluster (2) was termed 'anti-adipogenic progenitor' and corresponds to the Areg cluster.

[h]First, four FAP-clusters were identified based on scRNAseq to define the whole WAT heterogeneity. Subclustering analysis revealed eight distinct clusters, but DEGs were not displayed in the supplementary material. According to previous results, we assumed the association between both subclusters and assigned the eight subcluster to FAP1–4: FAP1–cluster (0), (4), (5); FAP2–cluster (3), (7); FAP3–cluster (1); FAP4–cluster (2), (6).

[i]The authors declared this cluster as 'uncommitted adipose progenitors,' following our nomenclature, we name this subset UMP.

[j]The authors declared this cluster as 'stem cell population enriched in adipogenic inhibitors,' following our nomenclature, we name this subset Areg.

[k]The authors analysed samples from SAT, VAT and subcutaneous leg AT. Although subcutaneous leg AT is typically classified as a regional subtype of SAT, the authors identified specific clusters and marker genes in subcutaneous leg AT and therefore treated it as a distinct depot throughout their analyses. Consequently, we decided to maintain this separation.

[l]Sample numbers (total *n*=126) were calculated according to Supplementary Tables 1 and 2.

[m]Specific cluster for mesocolic and perirenal AT, not observed in SAT or VAT

[n]Genes were mentioned in the study to define the eight clusters.